**Ghaneya, Abdel Halim A.**

SOME STUDIES ON THE VANADIUM-CARBON SYSTEM

*Iowa State University* PH.D. 1984

PLEASE NOTE:

In all cases this material has been filmed in the best possible way from the available copy. Problems encountered with this document have been identified here with a check mark __√__.

1. Glossy photographs or pages _____
2. Colored illustrations, paper or print _____
3. Photographs with dark background __√__
4. Illustrations are poor copy _____
5. Pages with black marks, not original copy _____
6. Print shows through as there is text on both sides of page _____
7. Indistinct, broken or small print on several pages __√__
8. Print exceeds margin requirements _____
9. Tightly bound copy with print lost in spine _____
10. Computer printout pages with indistinct print _____
11. Page(s) _____ lacking when material received, and not available from school or author.
12. Page(s) _____ seem to be missing in numbering only as text follows.
13. Two pages numbered _____. Text follows.
14. Curling and wrinkled pages _____
15. Other _____

# Some studies on the V-C system

by

Abdel Halim A. Ghaneya

A Dissertation Submitted to the

Graduate Faculty in Partial Fulfillment of the

Requirements for the Degree of

DOCTOR OF PHILOSOPHY

Department: Materials Science and Engineering
Major: Metallurgy

Approved:

Signature was redacted for privacy.

In Charge of Major Work

Signature was redacted for privacy.

For the Major Department

Signature was redacted for privacy.

For the Graduate College

Iowa State University
Ames, Iowa

1984

TABLE OF CONTENTS


| | Page |
|---|---|
| 1. INTRODUCTION | 1 |
| 2. LITERATURE REVIEW | 4 |
| 2.1. Phase Relationships | 4 |
| 2.1.1. Vanadium-rich terminal solid solution | 4 |
| 2.1.2. $V_2C$ phase | 6 |
| 2.1.3. Zeta phase | 7 |
| 2.1.4. VC phase | 9 |
| 2.2. Crystal Structure Data | 17 |
| 2.3. Thermodynamic Properties | 22 |
| 2.3.1. Low temperature heat capacity | 22 |
| 2.3.2. High-temperature heat content and heat capacity | 24 |
| 2.3.3. Heat and entropy of formation | 28 |
| 2.3.4. Vaporization | 32 |
| 3. EXPERIMENTAL WORK | 34 |
| 3.1. Materials | 34 |
| 3.2. Alloy Preparation | 35 |
| 3.3. Heat Treatment | 36 |
| 3.4. Metallographic Analysis | 37 |
| 3.5. X-ray Analysis | 37 |
| 3.6. Chemical Analysis | 37 |
| 3.7. Thermal Analysis | 38 |
| 3.8. Solubility Study | 39 |
| 3.9. Thinning of 1.5 at. % C Specimens for Electron Microscope | 39 |
| 3.10. Residual Resistivity Ratio Measurements | 40 |

4. EXPERIMENTAL RESULTS AND DISCUSSION 41

4.1. Zeta phase Vanadium Carbide 41

4.1.1. Metallographic and x-ray analyses 41
4.1.2. Stoichiometry and structure of ζ phase 53
4.1.3. Formation or decomposition temperature 59

4.2. Solid Solubility of C in Vanadium 62

4.2.1. Solvus boundary 66
4.2.2. Heat of solution 71
4.2.3. Determination of maximum solid solubility 71

4.3. Redetermination of Composition and Temperature of VC-C Eutectic 73

4.4. Ordering of C in V-1.5 at. % C Alloy 76

4.5. Residual Resistivity Ratio Study 80

5. CONCLUSIONS 85

5.1. Proposed Phase Diagram of the V-C System 85

5.1.1. Pure vanadium 85
5.1.2. Vanadium-rich solvus 85
5.1.3. $V_2C$ phase 87
5.1.4. Zeta phase 87
5.1.5. VC phase 88
5.1.6. VC-C eutectic 89

6. SUMMARY 90

7. REFERENCES 91

8. ACKNOWLEDGMENTS 96

# 1. INTRODUCTION

Many of the carbides of the transition metals possess high melting points and high hardnesses, low evaporation rates and low vapor pressures at high temperatures, good corrosion resistance and high temperature strength. In addition, they have electrical, magnetic, and optical properties that are typical of metals. These characteristics put them in the class of technologically promising materials. For example, an alloy of the substoichiometry $V_6C_5$ has a compressive yield strength-to-density ratio of 400,000 in. at 1250° [1], and a two-phase alloy of $VC_{1-x}$ and TiC has one of the highest compressive yield strengths of any known material at 1800°C, 36,300 psi [2]. The alloy VC-25 at. % TiC is particularly promising for technical applications due to its strength at high temperatures and its low density. The TiC-VC alloys are used as high temperature structural materials in a range for which the conventional super-alloys are no longer applicable. A high carbon vanadium alloy with the trade name Carvan is produced by a solid-state reduction of vanadium oxide in a vacuum furnace. This alloy is sometimes used as a replacement for ferrovanadium as a vanadium additive to special steels. Vanadium forms a very hard carbon deficient monocarbide which resists solution in austenite and remains unchanged throughout heat treatment cycles. Accordingly, this gives the great wear resistance to steel. For these and other reasons, a study of the V-C system is of considerable interest.

Although the phase relationships for the V-C system have been investigated over many years, there is still considerable uncertainty

over several features of the phase diagram. These features include: the solid solubility of carbon in vanadium, the homogeneity ranges and structures of the $V_2C$ and VC phases, the type of melting of the VC phase, the temperature and composition of the VC-C eutectic, and the temperature and mechanism of formation of a third intermediate phase, identified as a zeta phase, $\zeta$.

The areas selected for this investigation were:

1. A comprehensive literature survey and critical evaluation of all available data on the V-C system.
2. An investigation of some uncertain areas of the V-C diagram. This includes: a) preparation and identification of the reported $\zeta$ phase vanadium carbide, b) a determination of solid solubility limits of the carbon in vanadium in the range of 1100-1500°C, c) redetermination of the VC-C eutectic temperature and composition, and d) attempts to confirm or refute possible existence of an ordered $V_{64}C$ compound.
3. A determination of the contribution of carbon to the residual resistivity of vanadium.

Carbon is often found in vanadium and is difficult to remove completely during the purification step. To determine small concentrations of impurities in ultra-high purity metal, measurement of the residual resistivity ratio (RRR) of the metal is an excellent technique for this purpose. However, it is necessary to know the individual contribution of the various impurity elements to the total RRR of the metal before the impurity concentrations can be determined.

Therefore, it was of interest to determine the specific contribution $\rho'_C$ of carbon to the RRR of vanadium as a part of this investigation.

# 2. LITERATURE REVIEW

Early work on the V-C system has been summarized by Kieffer and Braun [3], but Storms and McNeal [4] were the first to propose a detailed phase diagram. In 1968, Rudy et al. [5] proposed the diagram shown in Figure 1 that was a modified version of the Storms and McNeal diagram. Later, other investigators found order-disorder transition reactions and other modifications not shown in Figure 1.

## 2.1. Phase Relationships

The vanadium-carbon system is similar to the other group $\overline{V}$ A-C systems in that they all have compounds, $V_2C$, a $\zeta$-phase, and VC. One important difference in this system is that the VC phase in equilibrium with carbon terminates at the carbon-rich side near $VC_{0.9}$ rather than at the stoichiometric composition. Each phase will now be reviewed separately.

### 2.1.1. Vanadium-rich terminal solid solution

High purity vanadium does not show any phase changes at ambient pressures and at temperatures up to its melting point [6]. Values for the melting point of vanadium metal range from 1860 [7] to 1919°C [8], but the generally accepted value is 1910 $\pm$ 7°C [9]. At the eutectic temperature, 1650°C, the maximum solubility of carbon in vanadium has been variously reported as 8.8 at. % C [4], 5.5 at. % C [5], 5.0 at. % C [10], 4.0 at. % C [11], and 1.08 at. % C [12]. As is shown in Figure 1, the solid solubility decreases rapidly as the temperature is reduced [10]. It was reported that the solid solubility is below one

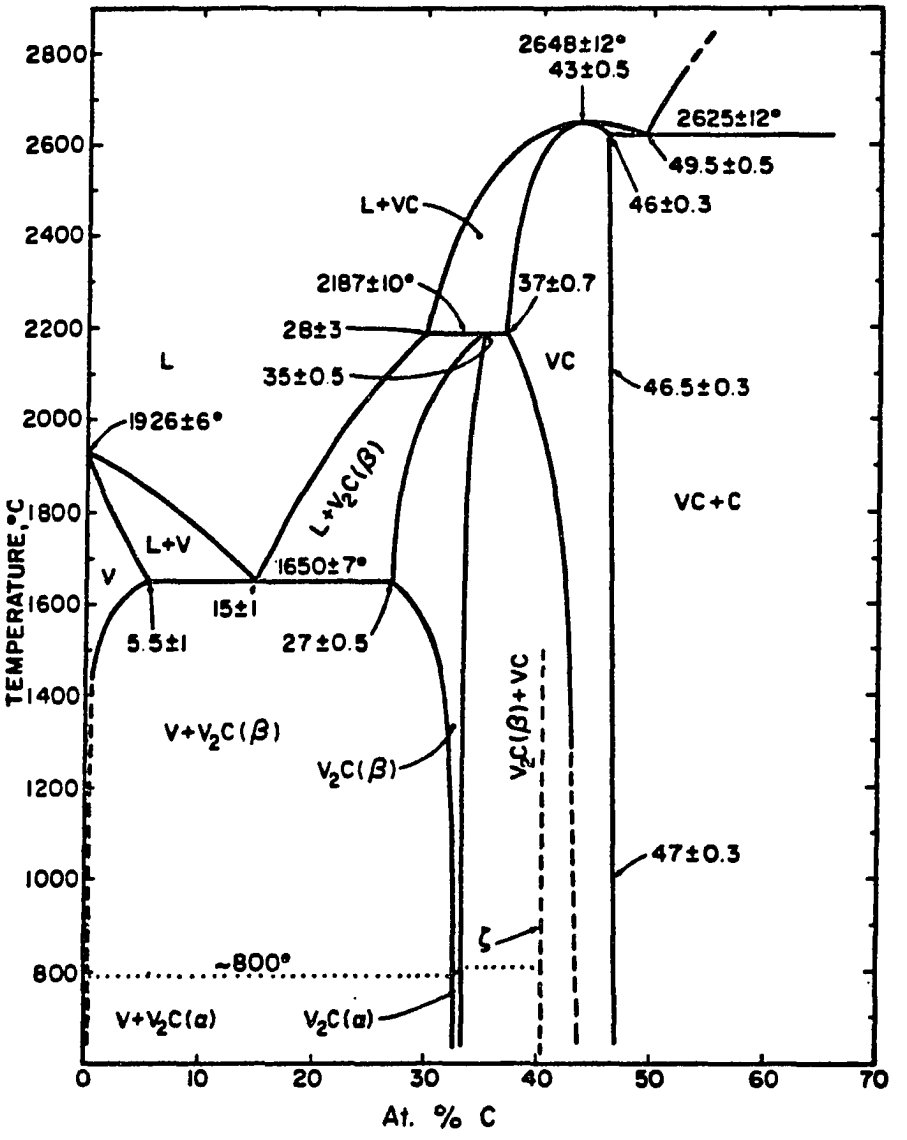


Figure 1. Phase diagram of V-C system (taken from Rudy et al. [5]

atomic percent at 1000°C [13-14] and ~ 0.13 at. % C at 700°C [12]. The dashed portion of the solvus in Figure 1 indicates a degree of uncertainty about this region of the diagram, however.

Thomas and Villagrana [15] have reported the possible occurrence of an ordered phase $V_{64}X$, in which X is an interstitial atom located in the 0, 1/2, 0 octahedral positions in the metal lattice similar to $Ta_{64}C$.

2.1.2. $V_2C$ phase

The vanadium solid solution phase and the subcarbide phase $V_2C$ form an eutectic at 15 at. % C and 1650 ± 7°C [5] as shown in Figure 1. Other investigators reported the eutectic point at 14.0 at. % C and 1650 ± 10 [11], and at 16.7 at. % C and 1630 ± 20°C [4]. The range of homogeneity of the $V_2C$ phase at 1650°C is shown in the diagram as extending from 27 to ~ 33 at. % C and melting peritectically at 2187°C. Others reported the range at the eutectic temperatures as 28.6 to 33.3 [16], 27 to 33.0 [13], 30 to 33.3 [11], and 29 to 33.3 at. % C [14]. Storms and McNeal [4] reported the homogeneity range of $V_2C$ at 1100°C from 32 to 33.3 at. % C and a peritectic melting temperature of 2165 ± 25°C. Reference [11] also reported peritectic melting at 2165°C.

A transformation from the high temperature hexagonal form (β) to an orthorhombic form (α) has been reported at about 800°C [5, 11, 17-21]. The transformation is associated with the ordering of the interstitial carbon atoms. There are also indications that at high temperatures the $V_2C$ phase has a hexagonal ordered structure [17-18]. Arbuzov et al. [21] performed x-ray analyses on single crystals on pseudo-single crystals of $V_2C$ of different compositions and heat treatments. They reported that

there is a change in the structure of the high temperature form of β with composition and heat treatment. At temperatures above 1600°C, $V_2C$ has a disordered hexagonal structure β, which becomes ordered hexagonal (β') in the range of 31 to 33 at. % C (see Figure 2a). The β phase transforms to an orthorhombic phase ($\beta_p$) with a composition corresponding to 33 at. % C. The alloys with compositions $\geq$ 35 at. % C show a hexagonal (β) structure down to room temperature. Khaenko and Fak [22] agree with the results of Arbuzov et al. [21] about changes in the $V_2C$ phase. The data of Arbuzov et al. [21] and Khaenko and Fak [22] are represented by the latter as shown in Figure 2a.

2.1.3. Zeta phase

Storms and McNeal [4] were the first to observe a carbide phase in the V-C system in the region between $VC_{0.60}$ and $VC_{0.74}$ below 1344°C. Their evidence came from unidentified lines in the x-ray diffraction powder patterns in addition to those due to VC and $V_2C$. The powder pattern of this phase is very similar to that of the zeta phase reported by Brauer and Lesser [23] and Lesser and Brauer [24] in the Nb-C and Ta-C systems. The x-ray patterns [11] of alloys near 40 at. % C showed $V_2C$ and VC lines accompanied by other lines which are identical with those of the ζ phase of Storms and McNeal [4]. Rasserts et al. [25] found zeta-phase lines in V-C alloys containing 37 to 39 at. % C and reported that it is isotypic with analogous compounds in the niobium- and tantalum-carbon systems. They tentatively assigned this compound the formula $V_3C_2$. Rudy et al. [5] observed a ζ phase as a distinct zone in a $V_2C$-graphite

diffusion couple. The diffusion couple was first heated to 2000°C for 10 minutes, followed by annealing at 1500°C for 162 hours. The presence of ζ phase is indicated as a dashed line in the Rudy diagram (Figure 1), since its exact temperature and composition were not known at that time. Yvon and Parthè [26] were the first to determine the crystal structure of ζ vanadium carbide by using single-crystal diffraction methods. They found it to have a hexagonal structure (trigonal symmetry) with lattice parameters a = 2.917 Å and c = 27.83 Å and c/a = 9.541. Also, they found systematic absences among the observed reflections at $-h+k+l \neq 3n$ which leads to the possible space groups R3, R3m, and $R\bar{3}m$. The symmetry of the structure is thus trigonal as is seen from the proposed structure of the ζ phase in Figure 3a. The structure is characterized by close-packed metal atoms with carbon atoms in the octahedral interstices. The shaded circles in Figure 3a corresponding to the point position 3(b) of the space group $R\bar{3}m$ are not occupied and hence, the ζ phase is proposed to be a carbon-deficient $V_4C_3$.

The mechanism of the ζ phase formation was studied by transmission electron microscopy by Billingham and Lewis [27] and by Van Landuyt and Amelinckx [28]. Billingham and Lewis observed large stacking faults in alloys whose compositions were close to the VC-$V_2C$ phase boundary. It was proposed that these stacking faults, bounded by Shockley partial dislocations, provide a nucleus for transformation of the cubic carbide to the β or ζ phases. Van Landuyt and Amelinckx [28] found supporting evidence for the above mechanism by the aid of electron diffraction data and dark field images. They also derived the lattice and orientation

relationship between the β and ζ phases and the cubic matrix which they represent schematically in Figure 3b. They found that β has $(0001)_{\beta}$ 11 $(111)_{matrix}$ and ζ has the trigonal plane $(111)_{\zeta}$ 11 $(111)_{matrix}$.

According to Rasserts et al. [25], Khaenko and Fak [22], and Storms et al. [29], the stoichiometric composition of the ζ phase was likely near $VC_{0.66}$. This is in agreement with the assignment of $V_4C_{2.67}$ as determined by Yvon and Parthè [26]. On the other hand, Billingham and Lewis [27] found x-ray lines that were predominantly those of the ζ phase plus additional lines of VC, but no $V_2C$ lines for an alloy of $VC_{0.65}$. Consequently, there appears to be some uncertainty in the exact stoichiometry of ζ. Storms et al. [29] looked for evidence for the thermal decomposition temperature of $VC_{0.66}$ by thermal analysis, but found no indication of an arrest between 1400 and 1800°C. The basis for the peritectoid horizontal at ~ 1475°C in Figure 2a is unclear.

### 2.1.4 VC phase

As mentioned earlier, there is a discrepancy in the melting nature of vanadium monocarbide. According to Storms and McNeal [4], it melts peritectically at 2650°C, whereas measurements by Rudy and Progulski [30] indicated a congruent melting point at 2648 ± 12°C and 43 ± 0.5 at. % C with the formation of an eutectic between the monocarbide and graphite at 2625°C and 49.5 ± 0.5 at. % C as shown in Figure 4. Results of other investigators [11, 29, 31] supported the congruent melting of VC. The ranges of homogeneity of vanadium monocarbide and data on the VC-C eutectic by various investigators are plotted on the enlarged portion of the Rudy diagram as shown in Figure 4. It appears that:

a) the carbon-rich boundary decreases slightly with temperature, while the vanadium-rich boundary of the phase is strongly temperature dependent,

b) the carbon-rich boundary is substoichiometric, and

c) vanadium monocarbide exists over a wide range of defect compositions [4, 13, 16, 32, 33].

An ordered arrangement of carbon vacancies was found at a composition of $V_8C_7$ by DeNovion et al. [34]. This is a cubic lattice of which the parameter is twice that of the rocksalt unit cell. This superstructure was also supported by a N.M.R. study by Froidevaux and Rossierr [35]. Volkova et al. [33] observed a rapid change in the enthalpy at the transition temperature, as well as lines in x-ray patterns which indicated the presence of $V_8C_7$. The order-disorder transition temperature was estimated to be 1100°C by Hollox [2] and determined to be 1112 $\pm$ 8°C by Emmons and Williams [36] by thermal analysis. Storms et al. [29] found a thermal arrest at 1130°C for alloys lying at or beyond the carbon-rich boundary of the VC phase. At that temperature, the formation of the ordered $V_8C_7$ phase along with precipitation of excess carbon was observed.

A different arrangement of carbon vacancies was found at the $V_6C_5$ stoichiometry by Venables et al. [37]. The symmetry of this structure corresponds to a trigonal class $P_{31}$ or $P_{32}$. An order-disorder transition at this composition was proposed between 1250 and 1300°C by Hollox and Venables [38], estimated at 1225°C by Govila [39] and determined to be 1184 $\pm$ 12°C by Emmons and Williams [36] by thermal analysis. A new type

of vacancy ordering with monoclinic symmetry was reported for the compound $V_6C_5$ by Billingham et al. [40]. This superstructure is closely related to, but different in symmetry from that proposed by Venables et al. [37]. Hiraga [41] used electron diffusion and electron microscopy in his investigation and the results revealed that the superstructure, $V_6C_5$, is monoclinic, in agreement with the results of Billingham et al.

Arbuzov et al. [21] reported an ordered monoclinic pseudocubic modification $\delta'_m$ which forms from the $\delta$ phase at ~ 1250°C by means of a metastable form $\delta''_m$. At about 900°C, they observed a second order phase transition $\delta'_m \rightarrow \delta'_c$, where $\delta'_c$ is an ordered cubic modification at low temperatures. This proposed relation between the different $\delta$ forms is shown in Figure 2a. Khaenko [42] used Khaenko and Fak [22] data and his results to represent the vanadium monocarbide phase region corresponding to its different modifications ($\delta'$, $\delta''$ and $\delta'_c$) as shown in Figure 2b. Figure 2c is an enlarged section of the system showing the boundaries of the two ordered phases $V_6C_5$ and $V_8C_7$ taken from Billingham et al. [43]. Billingham et al. [43] stated that there is a small free energy difference between the two structures at any particular temperature and composition within the shaded area in Figure 2c. Emmons and Williams [36] determined the latent heat of the ordering reactions for $VC_{0.833} \rightleftarrows (V_6C_5)$ and $VC_{0.875} \rightleftarrows (V_8C_7)$ as 23.85 $\pm$ 11.72 J/g-atom (5.7 $\pm$ 2.8 cal/g-atom) and 25.10 $\pm$ 10.04 J/g-atom (6.0 $\pm$ 2.4 cal/g-atom), respectively, using differential thermal analysis (DTA).

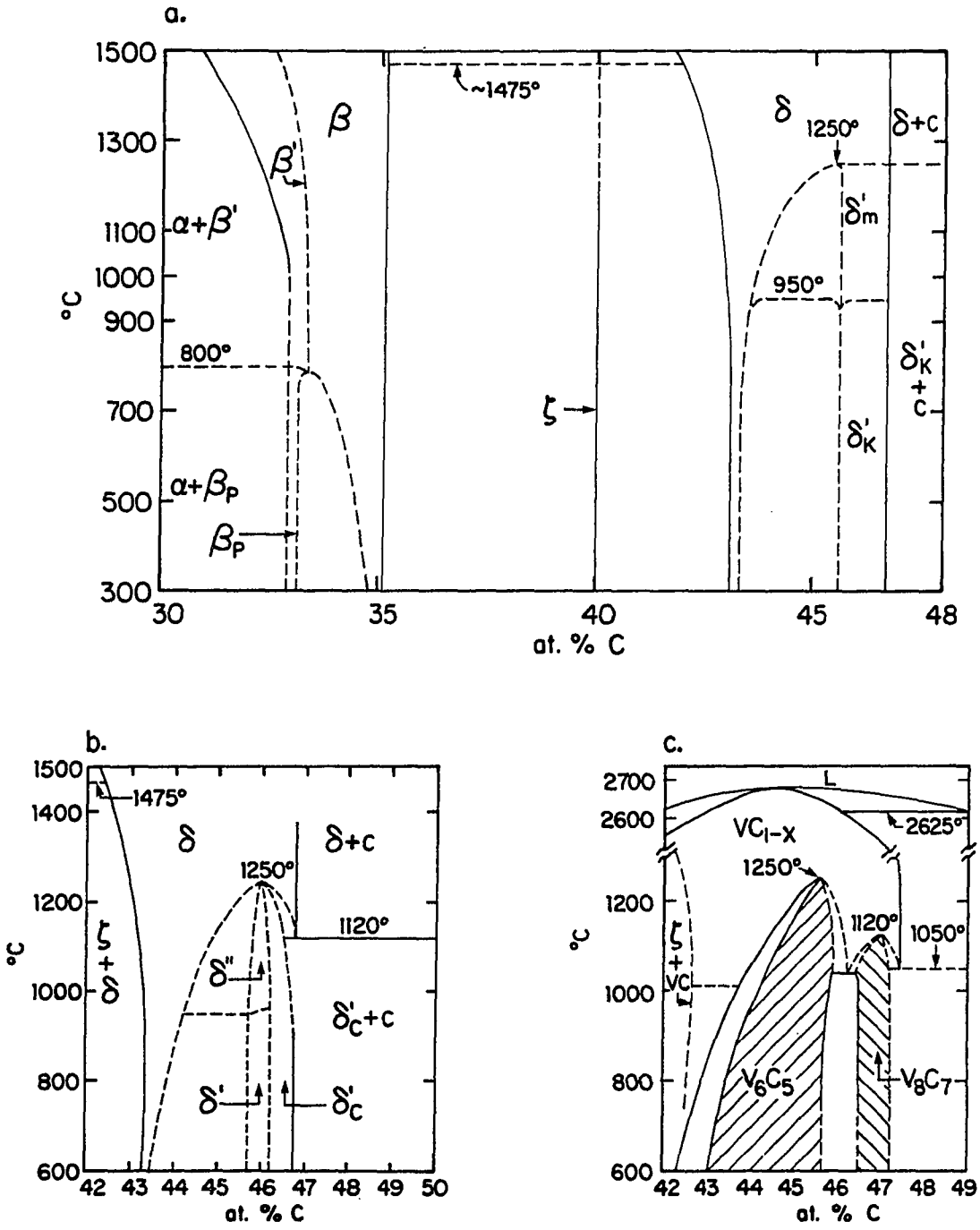


Figure 2. Portions of phase diagram of V-C system:
a. taken from Khaenko and Fak [22]
b. taken from Khaenko [42]
c. taken from Billingham et al. [40]

Figure 3a. Crystal structure of zeta phase (taken from Yvon and Parthè [26].

Coordinate of equivalent position based on hexagonal axes:

| | | | |
|---|---|---|---|
| 6 $V_1$ in | 6(C) | 00z | z ~ 1/8 |
| 6 $V_2$ in | 6(C) | 00z | z ~ 7/24 |
| | 6(C) | 00z | z ~ 5/12 |
| 8C in | 3(A) | 000 | |
| | 3(B) | 001/2 | |

Consider trigonal symmetry $R\bar{3}m$ and V is close-packed layers AB ABC AC ABC BC

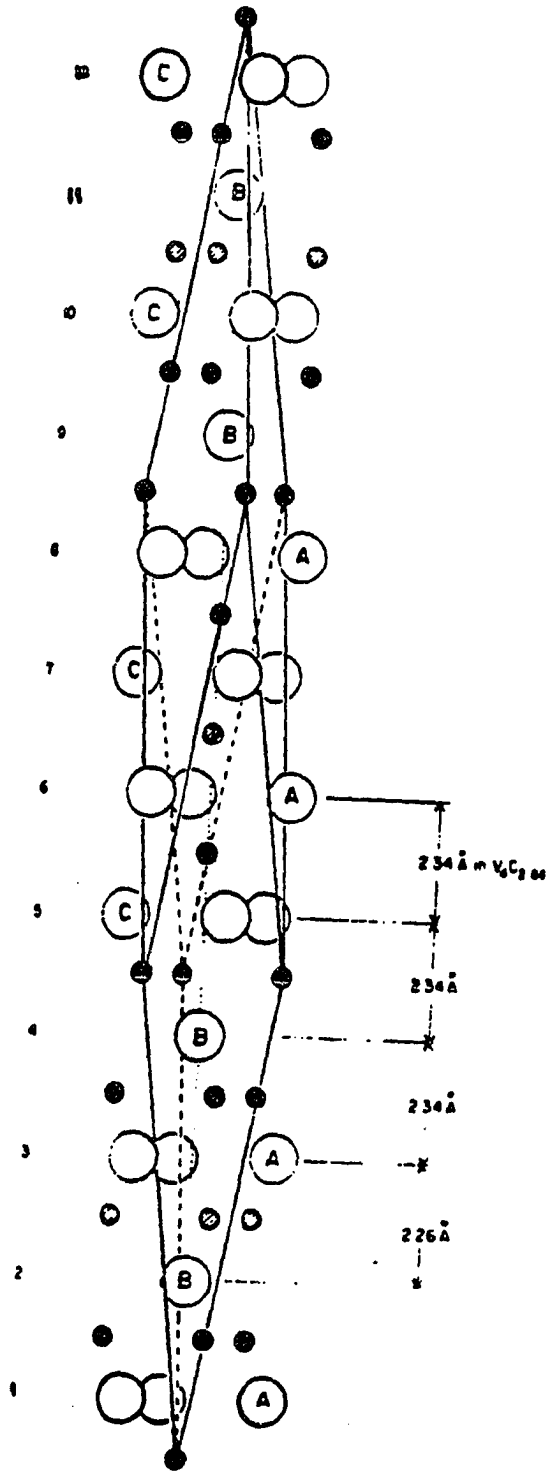
C
B
C
B
A
C
A
C
B
A
B
A
2.34 Å in $V_6C_{2.86}$
2.34 Å
2.34 Å
2.26 Å

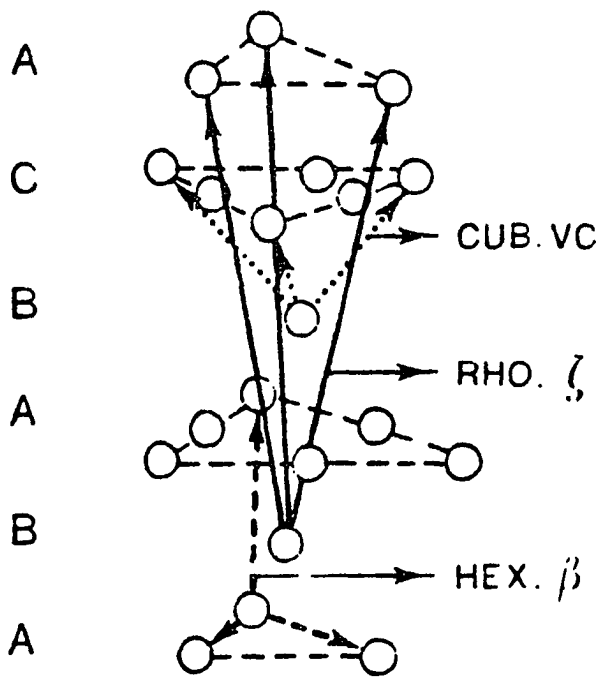


Figure 3b. Lattice relationship between ζ, $V_2C$ and VC (taken from Van Landuyt and Amelinckx [28])

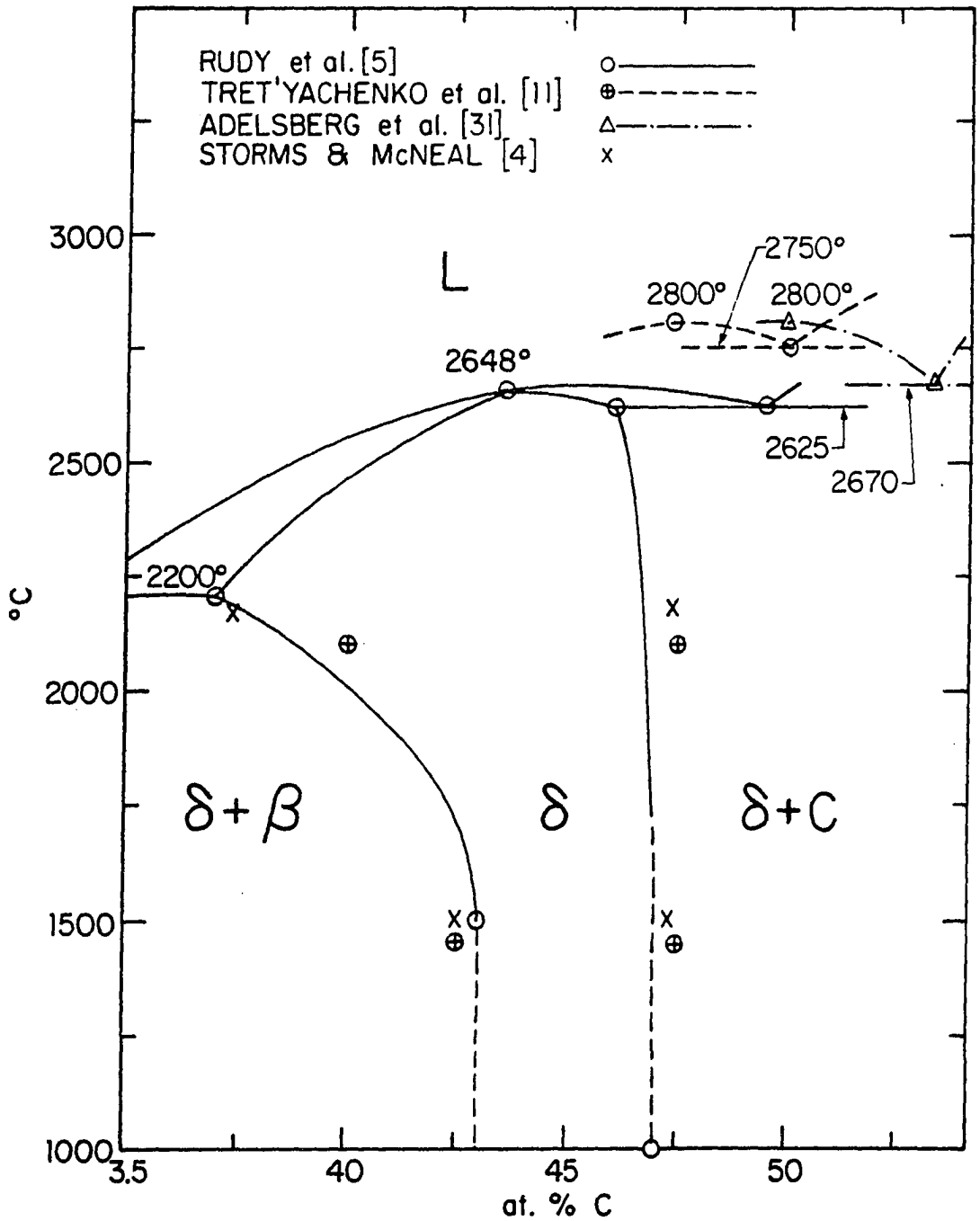


Figure 4. Boundaries of VC phase and eutectic point of VC + C constituent. (Based on literature data)

Khaenko and Fak [22] considered the type of phase transition for $\delta'_m \rightarrow \delta'_k$ (Figure 2a) as second order and Khaenko [42] did not indicate a definite type of transition between $\delta'$, $\delta''$ and $\delta'_c$ (Figure 2b). Billingham et al. [43] showed a first-order reaction for $V_6C_5$ and $V_8C_7$. This is in agreement with Shacklette and Williams [44, 45] who found evidence for the first-order results. Storms et al. [29] showed a first-order transition for $V_8C_7$.

Therefore, the type of the phase transition between δ-VC and its other modifications is still somewhat undecided. According to Billingham et al. [43], Emmons and Williams [36], and Shacklette and Williams [45, 46], the ordering of $V_6C_5$ and $V_8C_7$ are first-order reactions. Also, the data of Storms et al. [29] indicate that the transition of $V_8C_7$ is the same order. However, Khaenko and Fak [22] reported a second-order transition for $\delta'_m \rightarrow \delta'_c$. In a later paper [42], Khaenko stated that the type of phase transition (first or second order) remains a matter for discussion.

## 2.2. Crystal Structure Data

The crystal structure data of all reported phases in the V-C system are listed in Table 1.

The reported lattice parameters of β-$V_2C$ in Table 1 are plotted as a function of carbon content as shown in Figure 5. There is a regular increase in the a and c values as the stoichiometric composition of $V_2C$ (33.3 at. % C) is approached.

There is a great deal of confusion in the literature over the identification of the $V_2C$ phase. In the earlier work it is referred to

Table 1. Crystal structure data of reported phases in the V-C system

| Phase | Composition at. % C | Crystal Structure | Structure type | Space group | Lattice parameters, Å a | b | c | References |
|---|---|---|---|---|---|---|---|---|
| V | 0 | bcc | $W(A_2)$ | Im3m | 3.0321 | | | [6] |
| $\alpha$-$V_2C$ | 33 | orth | $\zeta$-$Fe_2N$ | $P_{bcn}$ | 4.575<br>11.490 | 5.760<br>10.06 | 5.020<br>4.55 | [19]<br>[20] |
| $\beta$-$V_2C$ | 32 | hex | $W_2C$ ($L'_3$) | $P6_3/mmc$ | 2.8855 | | 4.5705 | [4] |
| | 33 | | | | 2.9020 | | 4.5770 | [4] |
| | 27 | | | | 2.8810 | | 4.5470 | [13] |
| | 33 | | | | 2.9060 | | 4.5790 | [13] |
| | 29 | | | | 2.8700 | | 4.5460 | [14] |
| | 33.3 | | | | 2.8940 | | 4.5720 | [14] |
| $\beta_p$ | 35 | | | | 5.024 | | 4.5860 | [22] |
| $\beta_Q$-$V_2C_x$ | 31-33 | hex ordered | | $P6_322$ | 4.985 | | 4.5700 | [21] |
| $\zeta$-$V_4C_{3-x}$ | 40.2 | hex (hhcc) | $Sn_4P_3$ | $R\bar{3}m$ | 2.9185 | | 27.7880 | [26] |
| $\delta$-VC | 44.1 | cubic | NaCl (B1) | Fm3m | 4.136 | | | [13] |
| | 48 | | | | 4.182 | | | [13] |
| | 41.2 | | | | 4.158 | | | [14] |
| | 48 | | | | 4.168 | | | [14] |
| | 42.5 | | | | 4.1258 | | | [15] |

| | | | | | | | | |
|---|---|---|---|---|---|---|---|---|
| | 47.9 | | | | 4.168 | | | [16] |
| | 42.2 | | | | 4.131 | | | [4] |
| | 46.52 | | | | 4.1655 | | | [4] |
| | 46.81 | | | | 4.173 | | | [32] |
| | 42.5 | | | | 4.126 | | | [1] |
| | 47.5 | | | | 4.166 | | | [1] |
| $V_6C_5$ | 45.46 | hex | | $P3_1$ | 5.0654 | | 14.2371 | [38] |
| | 45.46 | monoclinic | B2 | | 5.090 | 10.180 | 8.820 | [41] |
| | | | | | $\gamma = 109.47°$ | | | |
| | 45.46 | orth | | | 3.6053 | 8.8311 | 28.8421 | [42] |
| $V_8C_7$ | 46.6 | cubic | | $P4_332$ | 8.33 | | | [34, 35] |

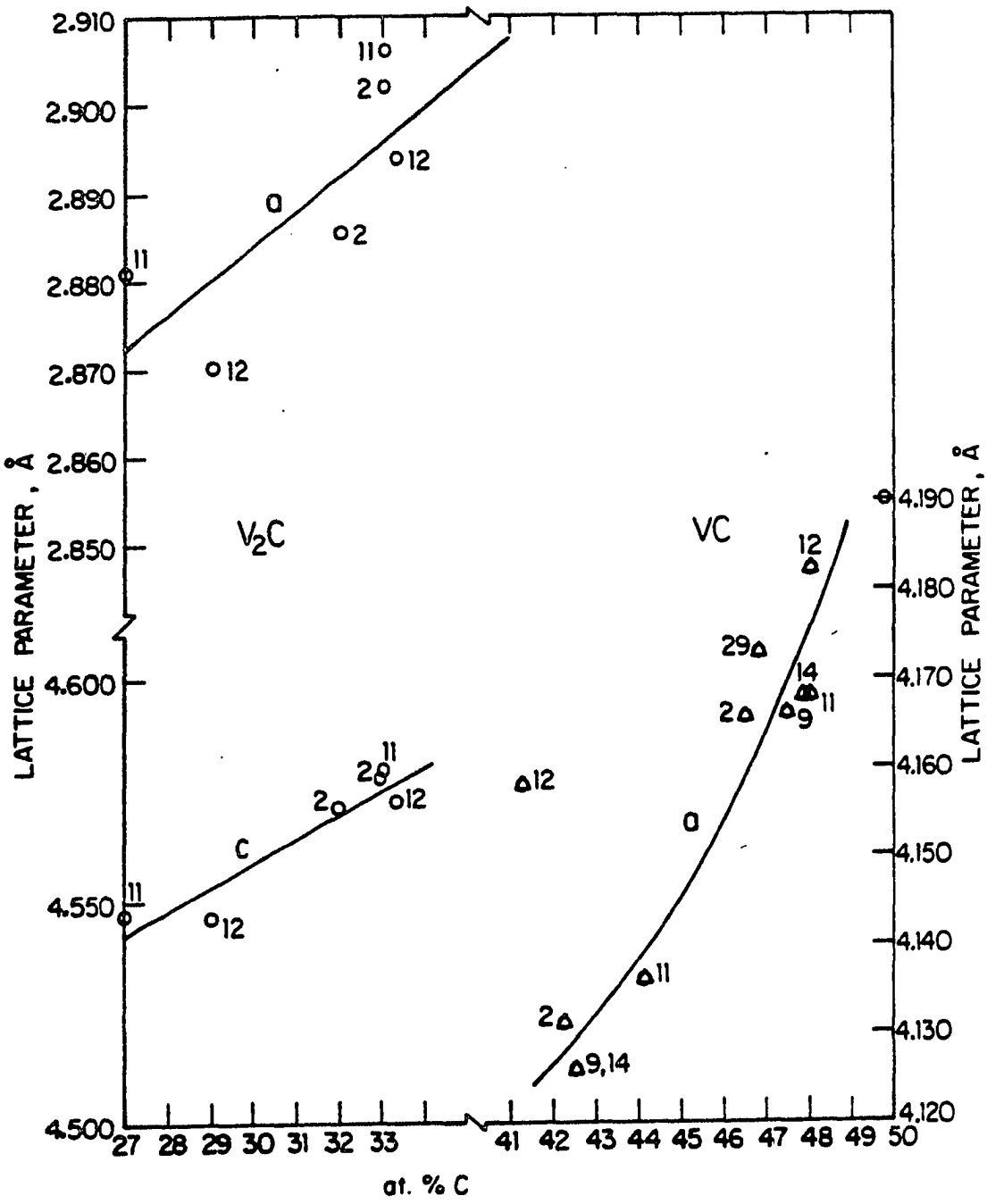


Figure 5. Relationship between lattice parameters of $V_2C$ and VC and their compositions. Numbers on graph refer to reference sources. (Based on data in Table 1)

as β, but as additional crystallographic forms appeared, they were given multiple designations. For example, the low temperature orthorhombic form has been identified by different investigators as $V_2C(\alpha)$, $\beta$-$V_2C$(< 800°C) and $\beta_p$. We shall refer to this phase as $\alpha$-$V_2C$ (ordered orthorhombic) and the high temperature form as $\beta$-$V_2C$ (random, hexagonal). For transformation from $\beta$-$V_2C$ to $\alpha$-$V_2C$, it is necessary to either anneal below 800°C or cool slowly (< 2°C/second) from a higher temperature. The transition is extremely sluggish when monocarbide is present [5]. Bowman et al. [46] used x-ray powder diffraction and neutron diffraction analyses to study the structure of $V_2C$, but they did not find any evidence of ordering, only the $L'_3$-type structure of $\beta$-$V_2C$ at room temperature. Khaenko and Fak [22] obtained a hexagonal form of $V_2C$ at $\leq$ 33 at. % C with $a = \sqrt{3}\, a_o = 5.024$ and $c = c_o = 4.586$ Å by quenching from 1600°C. This is identified in the table as $\beta_Q$. Arbuzov et al. [21] reported an ordered hexagonal $\beta'$-$V_2C_x$ of 31-33 at. % C.

Yvon and Parthè [26] obtained a hexagonal hhcc structure of $Sn_4P_3$-type for the $\zeta$-$V_4C_{3-x}$ compound. This corresponds to a superlattice with 12 stacked close-packed metal atom layers, as shown in Figure 3a.

The reported parameters of vanadium monocarbide in Table 1 are plotted as a function of carbon content as shown in Figure 5. The variation of the lattice parameter with the carbon content is nonlinear. The lattice parameter decreases as the monocarbide becomes more deficient in carbon.

The ordered compound $V_8C_7$, which is also identified as $\delta'_k$ and $\delta'_c$, has a cubic structure with a parameter double that of the NaCl-type structure. Another ordered compound $V_6C_5$ has been reported to have different types of structure: ordered hexagonal [37], monoclinic [40], and orthorhombic [41] as shown in the table. Different designations for this ordered phase are $\delta'$ and $\delta'_m$ which have been reported by other investigators [22, 42] to be monoclinic. This tends to support the monoclinic structure for $V_6C_5$.

## 2.3. Thermodynamic Properties

For a thermodynamic analysis of a material, three types of data are usually reported: the heat capacity from 0 to 298.15 K, the heat of formation at 298.15 K, and the high-temperature heat content referred to 298.15 K or some other reference temperature. Therefore, a summary of the heat capacity, enthalpy and entropy of formation, and the heat content are presented in this section. In addition, the vapor pressures or decomposition pressures and heat of vaporization or dissociation are also presented in the following subsections.

### 2.3.1. Low temperature heat capacity

Little work has been done on the low temperature heat capacity of the carbides of this system. Experimental work on the thermal capacity of the monocarbide at (52 - 297 K) was done by Schomate and Kelly [47]. Their data were actually for two-phase specimens. Hultgren et al. [48] calculated the selected values of $C_p$ after correcting the data to the stoichiometry of $VC_{0.88}$, as shown in Table 2.

Table 2. Low temperature $C^{o}_{p}$ for $VC_{0.88}$

| T, K | $C^{o}_{p}$ | |
|---|---|---|
| | J/K·gm-atom | cal/K·gm-atom |
| 10 | 0.008 | 0.002 |
| 25 | 0.14 | 0.034 |
| 50 | 1.13 | 0.27 |
| 75 | 3.18 | 0.76 |
| 100 | 5.48 | 1.31 |
| 125 | 7.70 | 1.84 |
| 150 | 9.62 | 2.30 |
| 175 | 11.38 | 2.72 |
| 200 | 12.85 | 3.07 |
| 225 | 14.14 | 3.38 |
| 250 | 15.27 | 3.65 |
| 275 | 16.32 | 3.90 |
| 298.15 | 17.20 | 4.11 |

Storms obtained $C^{o}_{p298.15\ K}$ = 32.308 J/mol-deg (7.722 cal/mol-deg) and $S^{o}_{298.15\ K}$ = 27.656 $\pm$ 0.13 J/mol-deg (6.61 0.03 cal/mol-deg) for $VC_{0.887}$ from the data of Schomate and Kelly [47]. Chernyaev et al. [49] experimentally determined the temperature dependence of $C_p$ of vanadium carbides of different compositions in the range 60 - 300 K by means of a low-temperature adiabatic calorimeter. Their measurements showed that the thermal capacities of all the $V_2C$ subcarbides ($VC_{0.46}$ and $VC_{0.53}$) and

the VC monocarbide ($VC_{0.712}$, $VC_{0.83}$ and $VC_{0.861}$) specimens increase monotonically with temperature. This indicates that the hexagonal and cubic vanadium carbides do not undergo phase transformations in this temperature range. They also found that the thermal capacities are markedly dependent on the composition; they increase rapidly with decreasing carbon content. It was found that $S^{o}_{V_2C}$ equals 17 J/g-atom. deg (4.063 cal/g-atom. deg) and $\Delta S^{o}_{VC}$ equals 12 J/g-atom. deg (2.87 cal/g-atom. deg), both at 298.16 K by interpolation and extrapolation, respectively, of the experimental data.

2.3.2. High-temperature heat content and heat capacity

Barin and Knacke [50] have listed $C^{o}_{p}$, $H^{o}$, $S^{o}$, and $G^{o}$ for $V_2C$ in the range of 298 to 2000 K, as shown in Table 3.

King [51] measured the heat content of $VC_{1.0}$ between 397 and 1611 K. After correcting for free carbon, these values were evaluated by Hultgren et al. [48] and Storms [52] to derive thermal functions for $VC_{0.88}$, as shown in Table 4. Storms' method of evaluation differs somewhat from that used by Hultgren et al. [48]. The latter fit King's data to the equation $H^{o}_{T} - H^{o}_{298.15\ K} = A + BT + CT^{2} + DT^{-1}$ by a least squares treatment. The heat capacity for many carbides, however, increases rapidly with temperature near the melting point. Therefore, Storms expanded the above equation to include a $T^{3}$ term to give a better fit for $C^{o}_{p}$ and $H^{o}_{T}-H^{o}_{298.15}$ of the carbides. The resulting equation by Storms is $H^{o}_{T}-H^{o}_{298.15\ K} = -3.0347 \times 10^{3} + 7.8928\ T + 2.4967 \times 10^{-3}\ T^{2} - 3.3282 \times 10^{-7}\ T^{3} + 1.3964 \times 10^{5} T^{-1}$. This equation was based on $C^{o}_{p_T}$ = 32.308 J/mol-deg (7.722 cal/mol-deg) and $H^{o}_{T} - H^{o}_{298} = 0$ at T = 298.15 K.

Table 3. Thermal functions of $V_2C$

| T (K) | $C^o_P$ | | $H^o_T$ | | $S^o_T$ | | $G^o_T$ | |
|---|---|---|---|---|---|---|---|---|
| | cal/mol-deg | J/mol-deg | kcal/mol | kJ/mol | cal/mol-deg | J/mol-deg | kcal/mol | kJ/mol |
| 298 | 14.034 | 58.718 | -35.2 | 147.3 | 14.3 | 59.831 | -39.464 | 165.117 |
| 300 | 14.073 | 58.881 | -35.174 | 147.2 | 14.387 | 60.195 | -39.490 | 165.226 |
| 400 | 15.595 | 65.259 | -33.683 | 140.9 | 18.665 | 78.094 | -41.149 | 172.167 |
| 500 | 16.570 | 69.329 | -32.072 | 134.2 | 22.256 | 93.119 | -43.200 | 180.749 |
| 600 | 17.329 | 72.505 | -30.376 | 127.1 | 25.346 | 106.047 | -45.584 | 190.724 |
| 700 | 17.985 | 75.249 | -28.610 | 119.7 | 28.067 | 117.432 | -48.257 | 201.907 |
| 800 | 18.588 | 77.772 | -26.781 | 112.1 | 30.509 | 127.650 | -51.188 | 214.171 |
| 900 | 19.159 | 80.161 | -24.893 | 104.2 | 32.731 | 136.947 | -54.352 | 227.469 |
| 1000 | 19.710 | 82.467 | -22.950 | 96.02 | 34.778 | 145.511 | -57.728 | 241.534 |
| 1100 | 20.284 | 84.718 | -20.952 | 87.66 | 35.682 | 153.478 | -61.302 | 256.488 |
| 1200 | 20.778 | 86.935 | -18.901 | 79.08 | 38.487 | 161.030 | -65.061 | 272.215 |
| 1300 | 21.302 | 89.128 | -16.796 | 70.28 | 40.151 | 167.992 | -68.993 | 288.667 |
| 1400 | 21.821 | 91.299 | -14.640 | 61.25 | 41.748 | 174.674 | -73.088 | 305.800 |
| 1500 | 21.821 | 93.485 | -12.432 | 52.02 | 43.272 | 181.050 | -77.340 | 323.591 |
| 1600 | 22.850 | 95.604 | -10.173 | 42.56 | 44.730 | 187.150 | -81.740 | 342.000 |
| 1700 | 23.361 | 97.742 | - 7.862 | 32.90 | 46.130 | 193.008 | -86.284 | 361.012 |
| 1800 | 23.871 | 99.876 | - 5.501 | 23.02 | 47.480 | 198.656 | -90.965 | 380.598 |
| 1900 | 24.380 | 102.006 | - 3.088 | 12.92 | 48.784 | 204.112 | -95.778 | 400.735 |
| 2000 | 24.887 | 104.127 | - 0.625 | 2.615 | 50.048 | 209.401 | -100.720 | 421.413 |

Table 4. Thermal functions of $VC_{0.88}$ according to Storms [52]

| T (K) | $H^\circ_T - H^\circ_{298}$ | | $C^\circ_p$ | | $S^\circ_T$ | | $-(F^\circ_T - H^\circ_{298})/T$ | |
|---|---|---|---|---|---|---|---|---|
| | cal/mol | J/mol | cal/mol-deg | J/mol-deg | cal/mol-deg | J/mol-deg | cal/mol-deg | J/mol-deg |
| 298.15 | 0 | 0 | 7.722 | 32.309 | 6.610 | 27.656 | 6.610 | 27.656 |
| 300 | 14.31 | 59.87 | 7.749 | 32.422 | 6.658 | 27.857 | 6.610 | 27.656 |
| 400 | 849.7 | 3555.12 | 8.858 | 37.062 | 9.053 | 37.878 | 6.929 | 28.991 |
| 500 | 1774 | 7422 | 9.581 | 40.087 | 11.11 | 46.484 | 7.565 | 31.652 |
| 600 | 2761 | 11552 | 10.14 | 42.426 | 12.91 | 54.015 | 8.309 | 34.765 |
| 700 | 3799 | 15895 | 10.61 | 44.392 | 14.51 | 60.710 | 9.083 | 38.003 |
| 800 | 4882 | 20426 | 11.03 | 46.150 | 15.96 | 66.777 | 9.853 | 41.225 |
| 900 | 6004 | 25121 | 11.41 | 47.739 | 17.28 | 72.230 | 10.61 | 44.392 |
| 1000 | 7162 | 29966 | 11.75 | 49.162 | 18.50 | 77.404 | 11.33 | 47.405 |
| 1100 | 8352 | 34875 | 12.06 | 50.459 | 19.63 | 82.132 | 12.04 | 50.375 |
| 1200 | 9573 | 40053 | 12.35 | 51.672 | 20.69 | 86.567 | 12.72 | 53.221 |
| 1300 | 10820 | 45271 | 12.61 | 52.760 | 21.69 | 90.751 | 13.37 | 55.940 |
| 1400 | 12100 | 50626 | 12.86 | 53.806 | 22.64 | 94.726 | 14.00 | 58.576 |
| 1500 | 13390 | 56024 | 13.07 | 54.685 | 23.53 | 98.450 | 14.60 | 61.086 |
| 1600 | 14710 | 61547 | 13.27 | 55.522 | 24.38 | 102.01 | 15.19 | 63.555 |
| 1700 | 16050 | 67153 | 13.45 | 56.275 | 25.19 | 105.40 | 15.75 | 65.898 |
| 1800 | 17400 | 72802 | 13.60 | 56.902 | 25.96 | 108.62 | 16.30 | 68.199 |
| 1900 | 18770 | 72802 | 13.60 | 56.902 | 25.96 | 108.62 | 16.30 | 68.199 |
| 2000 | 20150 | 84308 | 13.85 | 57.948 | 27.41 | 114.68 | 17.34 | 72.551 |

| | | | | | | | | |
|---|---|---|---|---|---|---|---|---|
| 2100 | 20150 | 84308 | 13.94 | 58.325 | 28.09 | 117.53 | 17.83 | 74.601 |
| 2200 | 22930 | 95939 | 14.02 | 58.660 | 28.47 | 120.25 | 18.31 | 76.609 |
| 2300 | 24340 | 101839 | 14.02 | 58.660 | 28.47 | 120.25 | 18.31 | 76.609 |
| 2400 | 25750 | 107738 | 14.10 | 58.994 | 29.96 | 125.35 | 19.24 | 80.5 |
| 2500 | 27160 | 113637 | 14.11 | 59.036 | 30.54 | 127.78 | 19.68 | 82.341 |

Volkova et al. [53] also measured the heat content of vanadium monocarbide, but their values are rather high and the resulting heat capacity of > 67 J/mol-deg (> 16 cal/mol deg) would be greater than for similar transition metal carbides which leaves some doubt concerning the accuracy of the measurements or the purity of the sample used.

2.3.3. Heat and entropy of formation

The reported values for the $\Delta H^{o}$ and $\Delta S^{o}$ of formation of $V_2C$ are listed in Table 5.

The data of Alekseev and Shvartsman [54] shown in Table 5 were determined using the following equilibrium $V_2C_{(s)} + 2H_{2(g)} = CH_{4(g)} + V_{(s)}$ in the temperature range of 973 - 1273 K. Volkova et al. [53] investigated several compositions of $V_2C_{1-x}$, and obtained the relation $\Delta H^{o}_{298.15}(V_2C) = -(10.1 + 12.8\ C/V) \pm 0.6$ K cal/mole where C/V is the ratio of atomic percentages of carbon to vanadium. Worrel [55] used an empirical relationship $\frac{\Delta H^{o}_{M_2C}}{\Delta H^{o}_{MC}} = 1.375 \pm 0.012$, where the $\Delta H^{o}$ quantities are calorimetric values of the groups V and VI metal carbides, to estimate $\Delta H^{o}_{298}$ of $V_2C$. Reznitskii [56] applied the Kireev comparative calculation of thermodynamic properties which states that $\Delta H^{o}_{x} = \alpha \Delta H^{o}_{y}$ where x and y are two similar reactions at the same temperature and $\alpha$ is a coefficient that is independent of temperature over a limited range. Reznitskii used $\Delta H^{o}_{298}(NbX)/\Delta H^{o}_{298}(VX) = 1.15 \pm 0.04$ where X is either the oxide or chloride ion for his estimation of $\Delta H^{o}_{298}(V_2C)$. Pillai and Sundareson [57] used a solid state galvanic cell:

Table 5. Thermodynamic properties of $V_2C$

| Method | $\Delta H^o$ | | $\Delta S^o$ | | References |
|---|---|---|---|---|---|
| | kcal/mol | kJ/mol | cal/mol-deg | J/mol-deg | |
| Manometric | -11.5 ± .5 | -48.12 ± 2.1 | 0.49 | 2.05 | [54] |
| Calorimetric | -16.5 ± 0.6 | -69 ± 2.5 | | | [53] |
| Theoretical calculation | -35.2 ± 0.5 | -147.3 ± 2.1 | -1 ± 1 | -4.18 ± 4.18 | [55] |
| Theoretical calculation | -40.0 ± 2.0 | -167.4 ± 8.4 | | | [56] |
| EMF | -41.92 | -175.4 | ~0 | ~0 | [57] |

V, $VF_3/CaF_3/VF_3$, $V_2C$, C to obtain $\Delta G^o(V_2C)$ as a function of temperature in the temperature range of 770 - 850°C. They used the $C^o_p$ values of Barin and Knacke [50] for their calculation of $\Delta H^o(V_2C)$ and since the latter have not specified the mode of calculation of these $C^o_p$ and $S^o$ values, the values of $\Delta H^o_{298}(V_2C)$ by Pillai and Sundareson must be considered as approximate. Also the value $\Delta H^o_{298}(V_2C)$ = -175.39 kJ/mol (-41.92 kcal/mol) obtained from EMF measurements is far different from the other experimental values and much closer to the theoretical values.

In Table 6, the most recent values of the thermodynamic properties of vanadium monocarbide are listed.

As is seen from the table, the reported value of -179.91 kJ/mol for $VC_{0.91}\ O_{0.04}$ by Gurevich [58] is much higher than the other values obtained by a similar calorimetric method. Even if it is assumed that the combustion of vanadium carbide is incomplete due to a liquid film of $V_2O_5$ being formed on the surface of the carbide particles or that the product of combustion gives a mixture of lower oxides in addition to the $V_2O_5$, it is difficult to explain this large difference in the calorimetric data. With the exception of Gurevich's results, there is good agreement between the results obtained by the calorimetric, Knudsen effusion and equilibrium pressure methods which all give values in the range of 95 - 106 kJ/mol (22.7 - 25.4 kcal/mol).

Volkova *et al.* [53] obtained the relation $\Delta H^o_{298}(VC_x)$ = (11.5 + 15.8 C/V) $\pm$ 1.6 kcal/mol for the monocarbide phase where C/V is the atom ratio of carbon to vanadium. Worrel and Chipman [59]

Table 6. Thermodynamic data of $VC_x$

| Method | $VC_x$ | $\Delta H^o$ kcal/mol | $\Delta H^o$ kJ/mol | $\Delta S^o$ cal/mol-deg | | References |
|---|---|---|---|---|---|---|
| Calorimetric | $VC_{0.91}C_{0.04}$ | -43 | -179.91 | | | [58] |
| (direct combustion) | $VC_{1.05}O_{.05}$ | -40 | -167.63 | | | [58] |
| Measuring $P_{CO}^{eqm}$ (CO-graphite-oxide-carbide) | $VC_{0.88}$ | -24.1 ± 0.7 | -100.83 ± 3 | | | [59] |
| Calorimetric (direct combustion) | ? | -24.35 ± 0.4 | -101.88 ± 1.67 | | | [60] |
| Measuring $P_v^{eqm}$ ($P_v$ over VC) | | -22.7 ± 5 | -94.98 ± 20.9 | | | [61] |
| Calorimetric (bomb calorimetry) | | -25.4 ± 1.6 | -106.27 ± 6.7 | | | [53] |
| Knudsen effusion | $V_8C_7$ | -25.0 ± 0.4 | -.04.6 ± 1.67 | ~0 | ~0 | [29] |

calculated the heat of formation of $VC_{0.88}$ by measuring the CO pressure over $VC_{0.88}$ in equilibrium with $V_2O_5$ + C between 1200 and 1300°C. Fujishiro and Gokcen [61] measured the equilibrium pressure of $V_{(g)}$ over $VC_{(s)} + C_{(graphite)}$ in the range of 2346 - 2545 K by means of a graphite Knudsen cell. Their results may be expressed by $\log P_v(atm) = -30,700/T + 7.63$ in the range of 2400 ± 200 K. Storms et al. [29] determined the vanadium activity and the partial molar enthalpy of vaporization as a function of temperature between 1600 and 2200 K using a mass spectrometer. From a Gibbs-Duhem integration, the activity and partial enthalpy of carbon were determined and these values were combined to obtain the entropy and enthalpy of formation.

### 2.3.4. Vaporization

All alloy compositions studied by Storms and McNeal [4] lost measurable amounts of vanadium when heated in a vacuum above 1800 K and therefore, an inert atmosphere was required to suppress these losses at high temperatures. Fujishiro and Gokcen [61] determined the pressure of $V_{(g)}$ over $VC_{0.88}$ + C between 2482 - 2513 K and their measurements were fit to the relation $\log P_v(atm) = -30,700\ T^{-1} + 7.63$. From thermochemical measurements, Storms [52] calculated the pressure of vanadium gas from which the following relation was derived: $\log P_v(atm) = -3.121 \times 10^4\ T^{-1} + 7.65$. It will be noted that this is very similar to the above relationship of Fujishiro and Gokcen.

Kohl and Stearns [62] reported the existence of two gaseous carbide phases, $VC_2$ and $VC_4$. They used the Knudsen effusion method in conjunction

with a mass spectrometer to study the vaporization of the vanadium-carbon system over the temperature range 2417 - 2603 K. They determined experimentally third-law enthalpies and combined them with published thermodynamic data to obtain the dissociation energy of $VC_{2(g)} = V_{(g)} + C_{2(g)}$ as 570 ± 20 kJ/mol (136.23 ± 4.78 kcal/mol) and a value of 1193 ± 22 kJ/mol (285.13 ± 5.6 kcal/mol) as the dissociation energy of the reaction $VC_{4(g)} = V_{(g)} + 2C_{2(g)}$. Atomization energies of $VC_{2(g)} = V_{(g)} + 2C_{(g)}$ and $VC_{4(g)} = V_{(g)} + 4C_{(g)}$ were calculated and their values are 1164.9 ± 18.2 kJ/mol (278.42 ± 4.35 kcal/mol) and 2382 ± 19.2 kJ/mol (569.31 ± 4.59 kcal/mol), respectively.

Storms et al. [29] used the same technique as Kohl and Stearns and measured the $VC_{2(g)}/V_{(g)}$ pressure ratio to determine the heat of formation of $VC_{2(g)}$ from $V_{(g)}$ and graphite. $\Delta H^{o}_{0}(VC_2)_g$ was determined as 259.41 ± 4.4 kJ/mol (62 ± 2 kcal/mol).

# 3. EXPERIMENTAL WORK

## 3.1. Materials

Two different sources of vanadium were used for the preparation of vanadium-carbon alloys. One was electrolytically refined metal [63] obtained from the Bureau of Mines and the other was alumino-thermically reduced (ATR) metal [64] (Lot 455) prepared at Ames Laboratory. Two different lots of the electrolytic grade material (Lots 303 and 167) were used in this study. The chemical analysis of these three lots is given in Table 7.

Table 7. Chemical analysis of vanadium metal, elements in at. ppm

| Elements | C | N | O | Al | Cr | Cu | Si | Fe | Na | Ta | W |
|---|---|---|---|---|---|---|---|---|---|---|---|
| Electrolytic | | | | | | | | | | | |
| Lot 303 | 51 | 4 | 51 | 6 | 6 | <4 | 27 | <18 | | | |
| Lot 167 | 251 | 36 | 111 | | ~15 | 10 | 10 | 6 | 11 | 28 | 67 |
| Al-Thermic reduced | | | | | | | | | | | |
| Lot 455 | 531 | 255 | 191 | <43 | | | 415 | | 67 | | |

Special spectroscopic electrode grade graphite or activated charcoal (Darrco G60) was used in this study as the source of carbon.

### 3.2. Alloy Preparation

Electrolytic vanadium (Lot 303) and spectroscopic grade graphite were melted together in an arc-melting furnace under a gettered argon atmosphere. First the vanadium metal was melted into a button and the graphite was then added in carefully weighed amounts to give the desired compositions. In the higher composition alloys, it was necessary to add the graphite during successive melting steps. Some of the graphite was placed beneath the vanadium button, while the remainder was placed on the edge of the copper mold where it could be pushed into the mold cavity between melts. Each alloy was then remelted three times inverting between melts to obtain a homogeneous alloy. The nominal and analyzed compositions of the alloys that were used for the $\zeta$ phase investigation are listed in Table 8.

Table 8. Nominal and analyzed chemical compositions of alloys for $\zeta$ phase study

| Alloy number | Nominal carbon content in at. % | Chemical analysis wt. % | Chemical analysis at. % |
|---|---|---|---|
| 1 | 36 | 10.68 | 33.68 |
| 2 | 37 | 11.87 | 36.38 |
| 3 | 38 | 12.90 | 38.60 |
| 4 | 39 | 12.94 | 38.69 |
| 5 | 40 | 13.41 | 39.67 |
| 6 | 41 | 13.83 | 40.49 |
| 7 | 42 | 15.08 | 42.98 |

For the solid solubility investigation, the ATR vanadium (Lot 455) was arc melted into a finger-shaped ingot that was then swaged into an 0.125 in. diameter rod. A section of this rod was used as a polycrystalline sample and the remaining portion was converted into a single crystal by electron beam float zone refining (EBFZR). The reason for using a single crystal specimen in the solubility study will be discussed in a later section.

In an attempt to prepare the ordered phase $V_{64}C$, ATR vanadium (Lot 455) and spectroscopic graphite were melted into an alloy button in an arc furnace.

For the residual resistivity ratio study, electrolytic-vanadium metal (Lot 167) was arc melted with very small graphite additions to obtain V-C alloys of 100, 200 and 300 wt. ppm carbon in addition to the base metal which contained 50 ppm C. The samples were prepared from these alloys by cold rolling and machining into 0.125" x 1" x 0.052" plates. Some samples were prepared from ATR vanadium (Lot 455) by the same procedure followed by annealing at 1000°C for 3 h.

### 3.3. Heat Treatment

The buttons for the $\zeta$ phase investigation were cut into segments. One segment of each alloy was encapsulated in a tantalum tube under a partial pressure of argon and annealed in an NRC vacuum furnace under $<10^{-6}$ torr at 1300°C for 100 hours. Alloys containing 36.38, 38.60, 39.67 and 40.49 at. % C were also annealed at 1300°C for 220 hours. An alloy containing 1.5 at. % C, the nominal composition of $V_{64}C$, was

annealed at 1000°C for 175 hours under a vacuum of $<10^{-5}$ torr and furnace cooled. Samples made from ATR vanadium (Lot 455) for RRR measurements were annealed at 1000°C for 3 hours in an annealing furnace.

### 3.4. Metallographic Analysis

Specimens were prepared for metallographic examination by mechanical grinding on 320 and 600 grit papers. This was followed by polishing on a wax lap using a slurry of Linde "A" alumina (0.3 μ) and then on a cloth (Mastertex) lap using a slurry of Linde "B" alumina (0.05 μ). The samples were etched using a chemical etchant of 50 parts $H_2O$, 10 parts HF, 5 parts $HNO_3$ and 5 parts $H_2SO_4$. The softer low-carbon alloys were mechanically ground and electropolished in a 6% perchloric acid-methanol solution at -70°C. The photomicrographs were taken on a Zeiss Axiomat Metallograph.

### 3.5. X-ray Analysis

X-ray diffraction patterns were taken by a Debye-Scherrer Camera using Ni-filtered $CuK_\alpha$ radiations ($\lambda\alpha_1$ = 1.54051 and $\lambda\alpha_2$ = 1.54433 Å). The brittle ζ phase alloys were crushed and ground to a fine powder in a small agate motar and the powder was packed in a quartz capillary tube. Following the x-ray study, the line positions on the film were measured and θ values and d spacings were then calculated.

### 3.6 Chemical Analysis

The carbon content of the alloys was determined by one of two methods depending on the carbon concentration. A gravimetric analysis was used for high carbon alloys. Combustion of the sample was carried

out in a stream of oxygen and the $CO_2$ gas product was absorbed on Ascarite. A Leco carbon analysis was used for samples containing low carbon concentrations. In this case, the $CO_2$ gas was collected on a molecular sieve trap. After replacing the oxygen with helium, the trap was electrically heated to evolve the $CO_2$ and the $CO_2$ concentration was determined from the thermal conductivity of the gas.

### 3.7. Thermal Analysis

Differential thermal analysis (DTA) was used in an effort to determine the decomposition temperature of the $\zeta$ phase carbide. After prolonged annealing of the 39.67 at. % C alloy for 220 hours at 1300°C to form a $\zeta$ phase, the specimen was crushed and sealed in a tantalum crucible. The lid of the crucible had a small tantalum tube insert for a thermocouple. This was positioned so the thermocouple could be in good physical contact with the sample. A tantalum specimen of the same mass was used as the reference specimen. Heating and cooling were carried out in an NRC vacuum furnace and the temperature of the sample $T_s$ and the temperature difference between the sample and the reference $\Delta T_s$ were recorded simultaneously by a two-pen recorder. Thermal analysis of another sample was performed by use of an advanced Differential Thermal Analyzer, Model 4045, Netzch, Gerätebu GmbH. This apparatus has a high and variable sensitivity with a temperature range of up to 1600°C.

To complement the results of the thermal analysis, specimens of the $\zeta$ phase were heated to 1350°C for 10 hours and 1450°C for a short time and cooled rapidly in the furnace. This was followed by microscopic

examination.

### 3.8. Solubility Study

Both polycrystalline and single crystal samples of pure vanadium (Lot 167) were surrounded with activated charcoal in a graphite crucible which was then sealed in a tantalum crucible. Samples were equilibrated at 1300, 1400, and 1500°C for 8, 5, and 3 hours, respectively. In addition, two single crystal samples were equilibrated at 1100 and 1200°C for 23 and 14 hours, respectively, and a pair (one of each single crystal and polycrystalline) was packed with charcoal in the same graphite crucible and equilibrated at 1400°C for 7.5 hours. The time to achieve equilibrium at each temperature was calculated by the following equation: $t = (X^2/4D)$, where $D = 4.7 \times 10^{-3} \exp^{-27300/RT}(65)$, and x is twice the average distance a solute diffuses in time, t. Samples were cooled at a mean rate of $300°/min.^{-1}$. After microscopic examination, the carbide layer was removed by machining on a lathe or by grinding. The sample was then degreased and electropolished for chemical analysis.

### 3.9. Thinning of 1.5 at. % C Specimens for Electron Microscope

After annealing the V-1.5 at. % C alloy, a section 0.203 mm thick was cut from it on a slow-speed diamond saw. Specimens 3 mm in diameter were punched from this thin section. These specimens were mechanically polished using 600 grit paper to remove rough edges and to assure uniform thickness. These specimens were then electropolished to perforation using a South Bay Jet Thinner (Model 550B), and a 20 vol. % $H_2SO_4$-methanol electrolyte at -30°C and 120 VDC. The resulting specimens

were cleaned in stirred, cold methanol at ~ 15°C for ~ 1/2 hour, then transferred to a Whatman #3 filter paper to absorb the methanol quickly.

The samples were examined in a JEOL 100 CX analytical electron microscope using a primary voltage of 120 KV and a double tilt stage (Model EM-BST for a side goniometer stage). The samples were examined in the CTEM (Conventional Transmission Electron Microscope) mode using normal imaging and SAD (Selected Area Diffraction) techniques. A few precipitates were examined in the microbeam diffraction mode resulting in spatial information in the range of 1500 Angstroms.

### 3.10. Residual Resistivity Ratio Measurements

The RRR for a series of low carbon alloys was determined using a four-terminal resistance measurement technique. The sample current was on the order of one ampere, which gave a voltage drop across the sample in the microvoltage range. The measurements were taken at 4.2 K with an applied magnetic field to suppress the superconductivity of the vanadium at that temperature.

# 4. EXPERIMENTAL RESULTS AND DISCUSSION

The experimental results are presented and interpreted. The results are also discussed and compared with the results of previous work in the same areas of investigation.

## 4.1. Zeta-phase Vanadium Carbide

### 4.1.1. Metallographic and x-ray analyses

Metallographic analyses of a series of alloys extending across the two-phase region between β and δ phases showed vanadium-carbon alloys containing 33.67 and 42.98 at. % C to be single phase microstructures after annealing at 1300°C for 100 h (Figures 6 and 7). The 33.67 at. % C alloy shown in Figure 6 is almost pure $V_2C$, while the 42.98 at. % C alloy (Figure 7) consists of a single phase of VC. The alloys of compositions 36.38 and 38.60 at. % C show a mixture of three phase structures as is seen from Figures 8 and 9, whereas samples of compositions 39.67 and 40.49 at. % C have the appearance of two phase microstructures only (Figures 10 and 11). However, x-ray diffraction data indicate that the latter two alloys are also a nonequilibrium mixture of three phases. Billingham and Lewis [27] have shown that laminar precipitates resembling those seen in Figures 10 and 11 are made up of a combination of ζ and $V_2C$.

The x-ray data for the above mentioned six alloys are listed in Tables 9-14. It will be noted that the data for the 33.67 and 42.98 at. % C alloys (Tables 9 and 14) show mostly $V_2C$ lines and only VC lines, respectively. As is seen from Tables 10 through 13, the 36.38, 38.60,

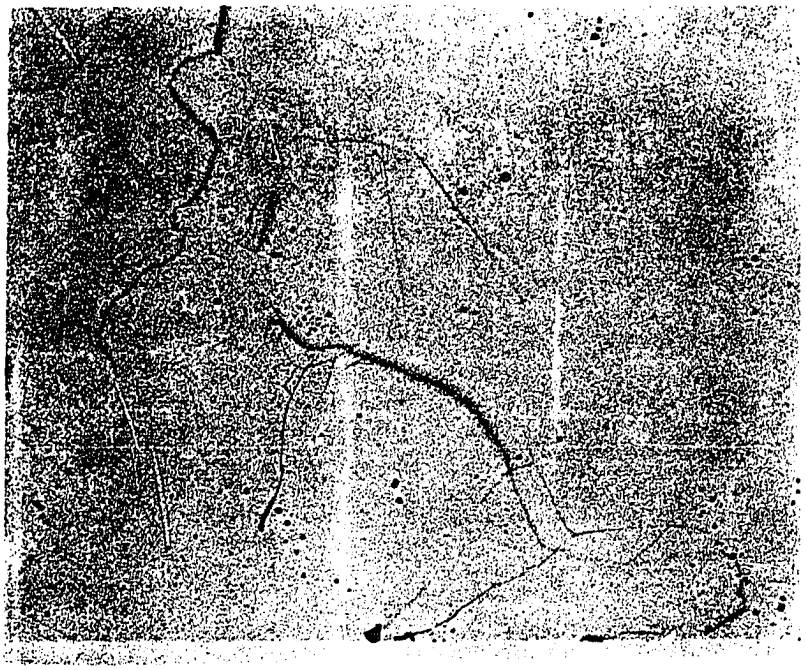

Figure 6. V-33.67 at. % C annealed at 1300°C for 100 h. Single-phase $V_2C$. Chemically etched, X150

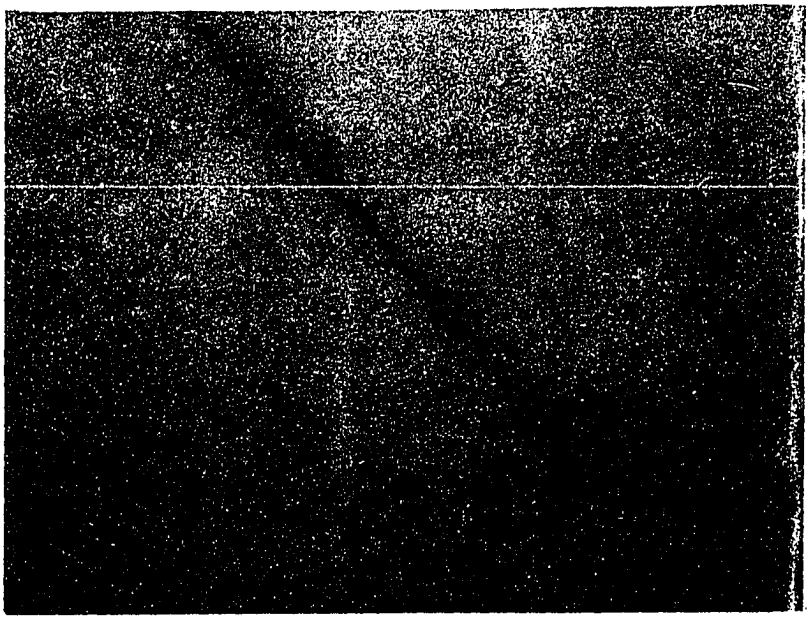

Figure 7. V-42.98 at. % C annealed at 1300°C for 100 h. Single-phase VC. Chemically etched, X150

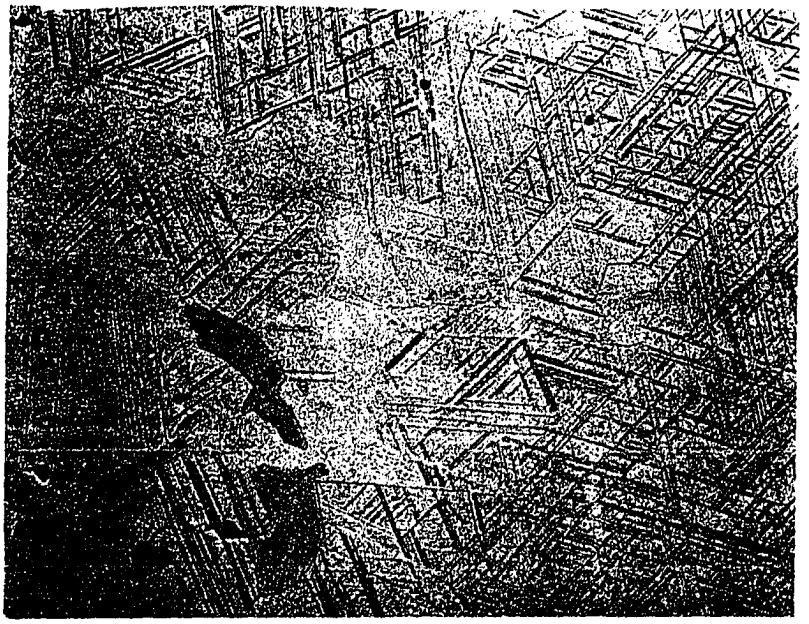

Figure 8. V-36.38 at. % C annealed at 1300°C for 100 h. Nonequilibrium mixture of $V_2C$ + VC + small amount of $\zeta$. Chemically etched, X250

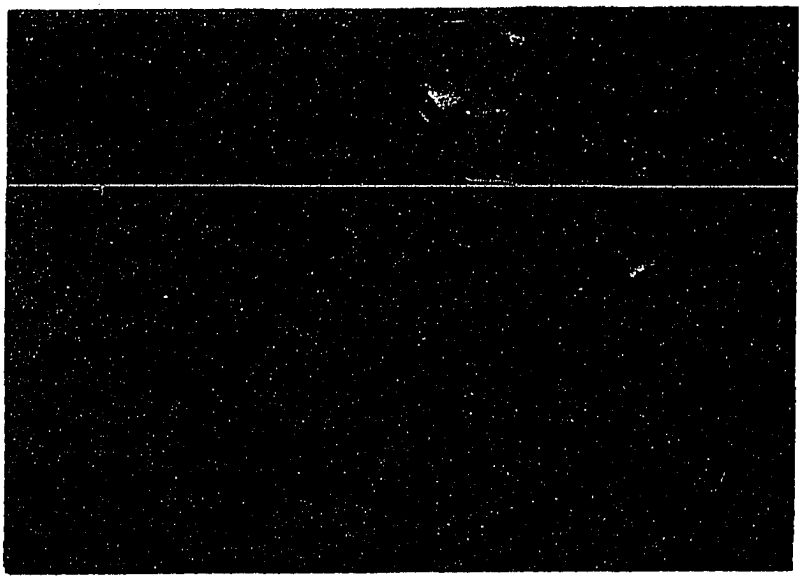

Figure 9. V-38.60 at. % C annealed at 1300°C for 100 h. Nonequilibrium mixture of $V_2C$ + VC + $\zeta$. Chemically etched, X400

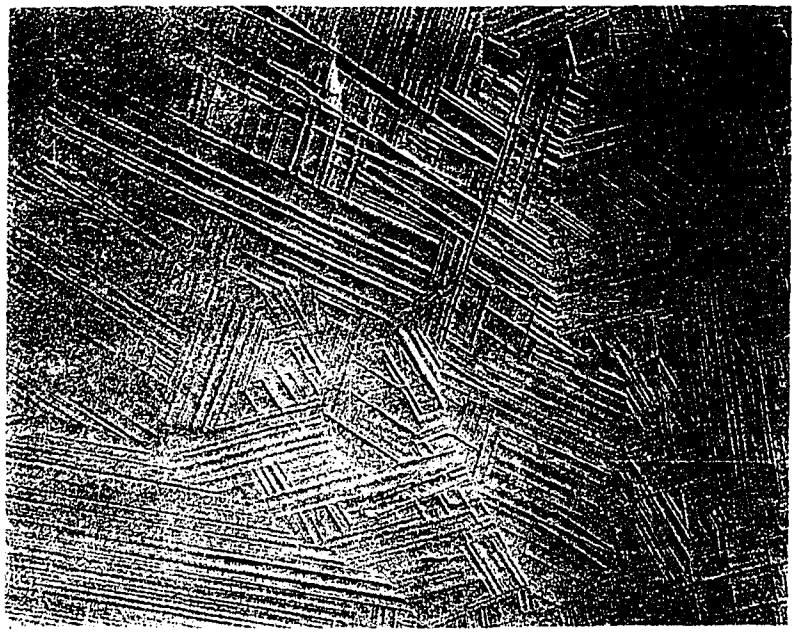

Figure 10. V-39.67 at. % C annealed at 1300°C for 100 h. Nonequilibrium mxiture of $\zeta$ + VC + small amount of $V_2C$. Chemically etched, X250

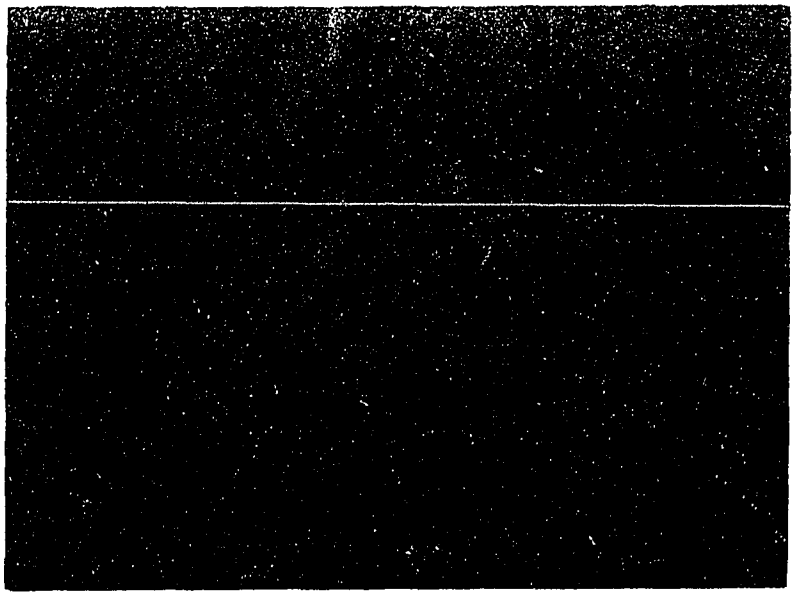

Figure 11. V-40.49 at. % C annealed at 1300°C for 100 h. Nonequilibrium mixture of $\zeta$ + VC + traces of $V_2C$. Chemically etched, X250

Table 9. X-ray data of V-33.67 at. % C annealed at 1300°C for 100 hours

| Line | Relative intensity $I/I_o$ | Reflection angle (2θ) | Plane spacing d, Å | Phases | hkl |
|---|---|---|---|---|---|
| 1 | LS | 35.94 | 2.4988 | $V_2C$ | 100 |
| 2 | VW | 36.84 | 2.4393 | ? | --- |
| 3 | W | 38.45 | 2.3417 | $V_2C$ | --- |
| 4 | LS | 39.70 | 2.2706 | $V_2C$ | 002 |
| 5 | VS | 41.15 | 2.1939 | $V_2C$ | 101 |
| 6 | S | 54.34 | 1.6886 | $V_2C$ | 102 |
| 7 | VW | 60.05 | 1.5408 | ζ | 01 $\underline{14}$ |
| 8 | VS | 64.51 | 1.4446 | $V_2C$ | 110 |
| 9 | VW | 67.22 | 1.3929 | ? | --- |
| 10 | S | 72.76 | 1.2929 | $V_2C$ | 103 |
| 11 | LS | 78.30 | 1.2212 | $V_2C$ | 112 |
| 12 | LS | 79.30 | 1.2083 | $V_2C$ | 201 |
| 13 | LS | 105.16 | 0.9708 | $V_2C$ | 210 |
| 14 | S | 112.03 | 0.9298 | $V_2C$ | 211 |
| 15 | S | 118.20 | 0.8986 | $V_2C$ | 114 |
| 16 | W | 122.78 | 0.8782 | $V_2C$ | 212 |
| 17 | S | 127.27 | 0.8605 | $V_2C$ | 105 |
| 18 | LS | 147.20 | 0.8022 | $V_2C$ | 113 |
| 19 | W | 156.44 | 0.7874 | $V_2C$ | 302 |

Table 10. X-ray data of V-36.38 at. % C annealed at 1300°C for 100 hours

| Line | Relative intensity $I/I_o$ | Reflection angle (2θ) | Plane spacing d, Å | Phases | hkl |
|---|---|---|---|---|---|
| 1 | VW | 36.33 | 2.4730 | ζ | 012 |
| 2 | S | 39.66 | 2.2727 | $V_2C$ | 002 |
| 3 | S | 41.48 | 2.1772 | $V_2C$ | 101 |
| 4 | S | 42.89 | 2.1087 | ζ | 107 |
| 5 | VW | 49.23 | 1.8512 | ζ | 10 $\underline{10}$ |
| 6 | W | 54.88 | 1.6732 | $V_2C$ | 102 |
| 7 | VW | 59.85 | 1.5456 | ζ | 01 $\underline{14}$ |
| 8 | VS | 64.19 | 1.4451 | $V_2C$ | 110 |
| 9 | VW | 69.03 | 1.3607 | ζ | 01 $\underline{17}$ |
| 10 | W | 73.07 | 1.2952 | $V_2C$ | 103 |
| 11 | VW | 76.70 | 1.2426 | ζ | 224 |
| 12 | W | 78.11 | 1.2236 | $V_2C$ | 112 |
| 13 | VW | 79.78 | 1.2022 | ζ | 027 + 210 |
| 14 | VW | 104.81 | 0.9730 | $V_2C$ | 210 |
| 15 | VW | 107.44 | 0.9564 | ζ | 02 $\underline{19}$ |
| 16 | VW | 109.81 | 0.9423 | VC | 133 |
| 17 | LS | 111.47 | 0.9329 | ζ | 20 $\underline{20}$ |
| 18 | W | 115.92 | 0.9096 | ζ | 11 $\underline{24}$ |
| 19 | W | 117.45 | 0.9019 | $V_2C$ | 212 |
| 20 | VW | 121.53 | 0.8836 | ? | 105 |
| 21 | W | 126.87 | 0.8620 | $V_2C$ | 105 |
| 22 | VW | 131.10 | 0.8469 | VC + ζ | 224 + 030 |
| 23 | W | 138.02 | 0.8258 | ? | --- |
| 24 | S | 145.28 | (0.8078) | $V_2C$ | 113 |
| 25 | LS | 148.46 | (0.8012) | $V_2C$ | 113 |
| 26 | LS | 153.16 | (0.7927) | VC | 115, 333 |
| 27 | VW | 154.62 | (0.7903) | VC | --- |
| 28 | LS | 155.98 | (0.7883) | $V_2C$ | 302 |
| 29 | VW | 157.44 | (0.7862) | $V_2C$ | 302 |

Table 11. X-ray data of V-38.60 at. % C annealed at 1300°C for 100 hours

| Line | Relative intensity $I/I_o$ | Reflection angle (2θ) | Plane spacing d, Å | Phases | hkl |
|---|---|---|---|---|---|
| 1 | W | 36.03 | 2.4636 | $V_2C$ | 100 |
| 2 | VW | 37.93 | 2.3726 | ζ + VC | 104 + 111 |
| 3 | S | 38.63 | 2.3310 | ? | --- |
| 4 | S | 40.98 | 2.2029 | $V_2C$ | 101 |
| 5 | S | 42.48 | 2.1278 | ζ | 107 |
| 6 | VW | 49.29 | 1.8489 | ζ | 10 $\underline{10}$ |
| 7 | VW | 53.79 | 1.7045 | $V_2C$ | 102 |
| 8 | VW | 59.29 | 1.5586 | ζ | 01 $\underline{14}$ |
| 9 | S | 63.80 | 1.4591 | ζ + VC | 110 + 022 |
| 10 | W | 68.15 | 1.3761 | ζ | 01 $\underline{17}$ |
| 11 | W | 72.30 | 1.3070 | $V_2C$ | 103 |
| 12 | VW | 74.81 | 1.2694 | ζ | 021 |
| 13 | S | 77.36 | 1.2336 | ζ | 205 |
| 14 | W | 79.51 | 1.2056 | ζ | 027 |
| 51 | W | 110.05 | 0.9409 | VC | 133 |
| 61 | LS | 112.15 | 0.9292 | ζ + VC | 20 $\underline{20}$ + 211 |
| 17 | LS | 116.45 | 0.9069 | ζ | 11 $\underline{24}$ |
| 18 | VW | 117.96 | 0.8728 | ? | --- |
| 19 | LS | 127.11 | 0.8611 | $V_2C$ | 105 |
| 20 | LLS | 131.92 | 0.8443 | ζ + VC | 030 + 224 |
| 21 | LLS | 137.79 | 0.8259 | ? | --- |
| 22 | W | 145.23 | (0.8079) | $V_2C$ | 113 |
| 23 | VW | 148.38 | (0.8013) | $V_2C$ | 113 |
| 24 | LS | 153.18 | (0.7926) | VC | 115, 333 |
| 25 | LLS | 154.63 | (0.7903) | VC | 115, 333 |
| 26 | W | 156.58 | 0.7874 | $V_2C$ | 302 |

Table 12. X-ray data of V-39.67 at. % C annealed at 1300°C for 100 hours

| Line | Relative intensity $I/I_o$ | Reflection angle (2θ) | Plane spacing d, Å | Phases | hkl |
|---|---|---|---|---|---|
| 1 | VW | 36.13 | 2.4865 | ζ + $V_2C$ | 012 + 100 |
| 2 | S | 37.83 | 2.3785 | ζ + VC | 104 + 111 |
| 3 | S | 39.30 | 2.2925 | ζ | 015 |
| 4 | VW | 41.08 | 2.1974 | $V_2C$ | 101 |
| 5 | S | 42.53 | 2.1258 | ζ | 107 |
| 6 | S | 43.88 | 2.0634 | VC | 002 |
| 7 | VW | 48.84 | 1.8651 | ζ | 10 $\underline{10}$ |
| 8 | VW | 59.24 | 1.5599 | ζ | 01 $\underline{14}$ |
| 9 | S | 63.95 | 1.4560 | ζ + VC | 110 + 220 |
| 10 | VW | 68.50 | 1.3699 | ζ | 01 $\underline{17}$ |
| 11 | W | 75.06 | 1.2657 | ζ | 021 |
| 12 | W | 76.71 | 1.2425 | ζ + VC | 204 + 113 |
| 13 | LS | 77.51 | 1.2317 | ζ | 205 |
| 14 | LS | 112.35 | 0.9281 | VC | 024 |
| 15 | LS | 113.55 | 0.9217 | ζ | 128 |
| 16 | LS | 116.50 | 0.9067 | ζ | 11 $\underline{24}$ |
| 17 | VVW | 127.76 | 0.8587 | $V_2C$ | 105 |
| 18 | VS | 132.32 | (0.8429) | ζ + VC | 030 + 224 |
| 19 | W | 133.17 | (0.8402) | ζ + VC | 030 + 224 |
| 20 | VW | 145.53 | (0.8011) | ζ + $V_2C$ | 21 $\underline{19}$ + 113 |
| 21 | W | 148.48 | (0.8011) | ζ + $V_2C$ | 21 $\underline{19}$ + 113 |
| 22 | W | 151.93 | (0.7947) | VC | 115, 333 |
| 23 | VW | 153.38 | (0.7923) | VC | 115, 333 |

Table 13. X-ray data of V-40.49 at. % C annealed at 1300°C for 100 hours

| Line | Relative intensity $I/I_o$ | Reflection angle (2θ) | Plane spacing d, Å | Phases | hkl |
|---|---|---|---|---|---|
| 1 | VW | 36.26 | 2.4779 | ζ + $V_2C$ | 012 + 100 |
| 2 | S | 37.99 | 2.3691 | ζ + VC | 104 + 111 |
| 3 | S | 39.06 | 2.3062 | ζ | 015 |
| 4 | VVW | 40.92 | 2.2059 | $V_2C$ | 101 |
| 5 | S | 42.39 | 2.1324 | ζ | 107 |
| 6 | S | 43.82 | 2.0662 | ζ + VC | 018 + 002 |
| 7 | VVW | 47.75 | 1.9049 | ? | --- |
| 8 | VW | 59.85 | 1.5456 | ζ | 01 $\underline{14}$ |
| 9 | S | 63.90 | 1.4569 | ζ + VC | 110 + 022 |
| 10 | VW | 68.43 | 1.3710 | ζ | 01 $\underline{17}$ |
| 11 | VW | 75.17 | 1.2641 | ζ | 021 |
| 12 | W | 76.71 | 1.2444 | ζ + VC | 024 + 113 |
| 13 | W | 77.67 | 1.2295 | ζ | 205 |
| 14 | VW | 109.04 | 0.9468 | VC | 133 |
| 15 | LLS | 112.29 | 0.9284 | VC | 024 |
| 16 | LLS | 113.45 | 0.9222 | ζ | 128 |
| 17 | LLS | 116.35 | 0.9074 | ζ | 11 $\underline{24}$ |
| 18 | VS | 132.27 | 0.8431 | ζ + VC | 030 + 224 |
| 19 | VW | 148.85 | 0.8004 | ζ | 21 $\underline{19}$ |
| 20 | LS | 151.56 | (0.7954) | ζ | |
| 21 | LS | 153.31 | (0.7924) | VC | 115, 333 |

Table 14. X-ray data of V-42.98 at. % C annealed at 1300°C for 100 hours

| Line | Relative Intensity $I/I_o$ | Reflection angle (2θ) | Plane spacing d, Å | Phases | hkl |
|---|---|---|---|---|---|
| 1 | VS | 37.77 | 2.3828 | VC | 111 |
| 2 | VS | 43.75 | 2.0695 | VC | 002 |
| 3 | VS | 63.75 | 1.4594 | VC | 022 |
| 4 | S | 76.53 | 1.2448 | VC | 113 |
| 5 | LS | 80.67 | 1.1912 | VC | 222 |
| 6 | LS | 108.65 | 0.9491 | VC | 133 |
| 7 | S | 113.03 | 0.9244 | VC | 024 |
| 8 | S | 131.57 | (0.8454) | (VC) | 224 |
| 9 | LS | 132.02 | (0.8439) | (VC) | 224 |
| 10 | S | 150.70 | (0.7969) | (VC) | 115, 333 |
| 11 | LS | 151.85 | (0.7948) | (VC) | 115, 333 |

39.67 and 40.49 at. % C alloys consist of various amounts of each phase. The proportional amounts of phases are $V_{2c} >> VC = \zeta$, $V_{2c} > \zeta >> VC$, $\zeta >> VC >> V_{2c}$ and $VC > \zeta >> V_{2c}$ from Tables 10 through 13, respectively.

Table 15 is a summary of the chemical analysis and phases present in the six alloys. From this, it is evident that equilibrium was not attained by this treatment. Therefore, those specimens consisting of a nonequilibrium mixture of $V_2C + \zeta + VC$ phases were given an additional 120 h anneal (1300°C for 220 h total). Following this prolonged annealing, the 36.38 and 38.60 at. % C alloys show approximately equal amounts of $\zeta$ and $V_2C$ (Figures 12 and 13). The microstructure of the 40.49 at. % C alloy shows platelike precipitates of $\zeta$ in a matrix of

Table 15. Chemical analysis and phases present from x-ray analyses after annealing at 1300°C for 100 h

| Alloy no. | Carbon content in at. % | Phases present |
|---|---|---|
| 1 | 33.7 | $V_2C$ |
| 2 | 36.4 | $V_2C + \zeta + VC$ |
| 3 | 38.6 | $V_2C + \zeta + VC$ |
| 4 | 39.7 | $VC + \zeta + V_2C$ |
| 5 | 40.5 | $VC + \zeta + V_2C$ |
| 6 | 43.0 | VC |

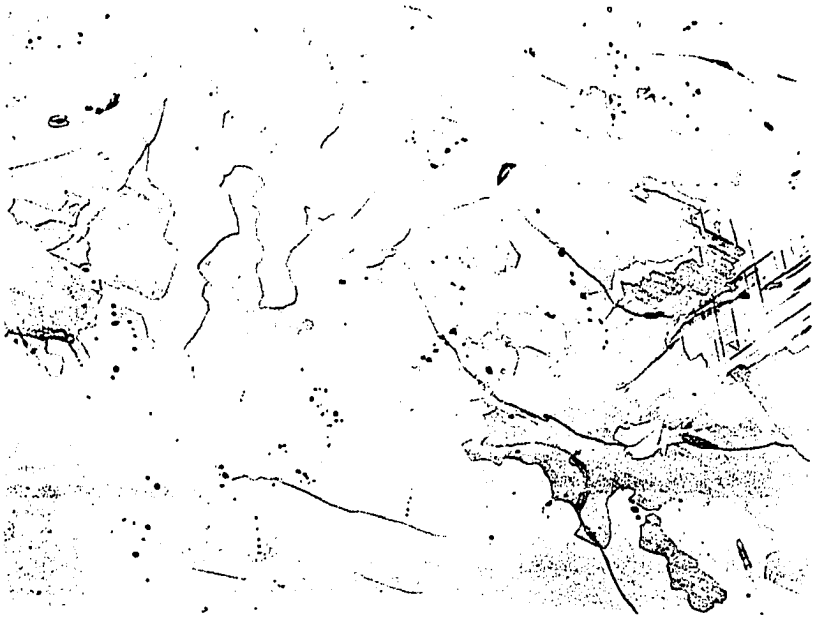

Figure 12. V-36.38 at. % C annealed at 1300°C for 200 h. Mixture of $\zeta$ and $V_2C$ in equal amounts. Chemically etched, X250

Figure 13. V-38.60 at. % C annealed at 1300°C for 220 h. Small amount of $V_2C$ in $\zeta$ matrix. Chemically etched, X250

VC (Figure 14). The 39.67 at. % C alloy is now almost completely single phase (Figure 15), indicating that it is close to equilibrium and also near the stoichiometry of ζ phase.

The x-ray data of these four alloys are listed in Tables 16-19. Tables 16 and 19 show the existence of x-ray diffraction lines of both $V_2C$ and ζ phases. The x-ray data of the 39.67 at. % C alloy shown in Table 18 show clearly that the alloy consists of the ζ phase except for a few weak VC lines, some of which are superimposed on ζ lines. Data for the 40.49 at. % C alloy in Table 19 show predominantly ζ along with strong VC reflections. So the x-ray analyses are in agreement with the metallographic analyses of these alloys.

### 4.1.2. Stoichiometry and structure of ζ phase

The x-ray data of the 39.67 at. % C alloy (Table 18) are identical to those obtained by Yvon and Parthè [26] for the front reflections for $V_4C_{3-x}$ ($x = 0.33$), with a random carbon atom arrangement. They did not include any high angle lines, however, so the indexing of these reflections has been done in Table 18. The indexing of the high angle ζ lines was obtained with the consideration that the systematic absences for the observed hkl reflections occur for $-h+k+l \neq 3n$. So, the hexagonal structure of ζ, as determined by Yvon and Parthè, was confirmed. The lattice parameters were determined from the x-ray data in Table 10 using the Latt Program by R. A. Jacobson to be $a = 2.9185 \pm 0.002$ Å and $c = 27.788 \pm 0.03$ Å.

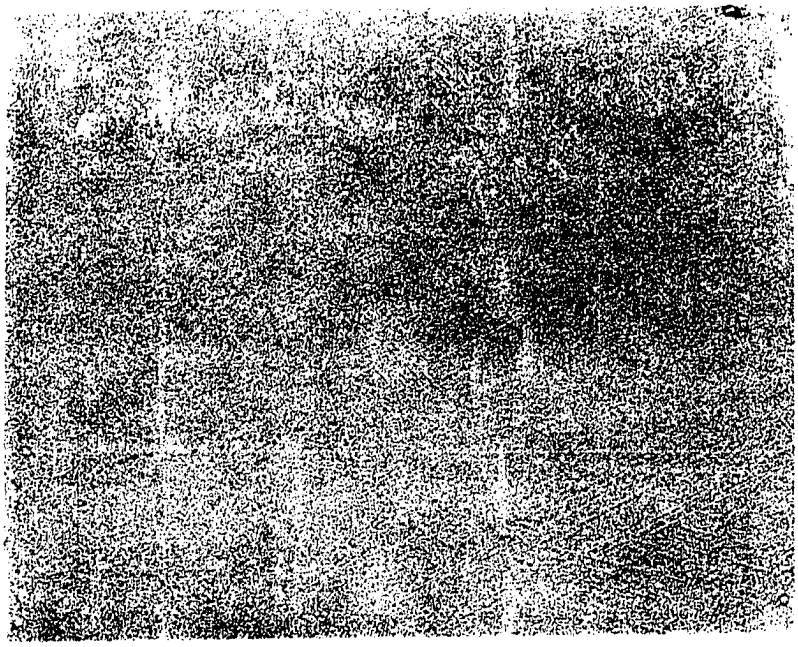

Figure 14. V-40.49 at. % C annealed at 1300°C for 220 h. Banded ζ in matrix of VC. Chemically etched, X250

Figure 15. V-39.67 At. % C annealed at 1300°C for 220 h. Nearly single-phase ζ. Chemically etched, X250

Table 16. X-ray data of V-36.38 at. % C annealed at 1300°C for 220 hours

| Line | Relative intensity $I/I_o$ | Reflection angle (2θ) | Plane spacing d, Å | Phases | hkl |
|---|---|---|---|---|---|
| 1 | VW | 35.75 | 2.5117 | $V_2C$ | 100 |
| 2 | LS | 39.56 | 2.2783 | $V_2C$ | 002 |
| 3 | S | 41.17 | 2.1927 | $V_2C$ | 101 |
| 4 | VW | 43.96 | 2.0596 | ζ | 018 |
| 5 | W | 54.54 | 1.6826 | $V_2C$ | 102 |
| 6 | VW | 68.70 | 1.3662 | ζ | 01 $\underline{17}$ |
| 7 | W | 72.66 | 1.3012 | ζ | 119 |
| 8 | VW | 77.91 | 1.2261 | ζ | 205 |
| 9 | VW | 79.07 | 1.2111 | ζ + $V_2C$ | 027 + 201 |
| 10 | VW | 105.34 | 0.9695 | ζ + $V_2C$ | 11 $\underline{24}$ + 210 |
| 11 | LS | 111.99 | 0.9299 | ζ | 20 $\underline{20}$ |
| 12 | VW | 116.31 | 9.9075 | ζ | 21 $\underline{10}$, 11 $\underline{24}$ |
| 13 | LS | 118.15 | 0.8986 | ζ | 12 $\underline{11}$ |
| 14 | VW | 122.92 | 0.8776 | ζ | 21 $\underline{13}$ |
| 15 | W | 126.63 | 0.8628 | ζ + $V_2C$ | 12 $\underline{17}$ + 105 |
| 16 | VW | 133.73 | 0.8383 | ζ | 21 $\underline{16}$ |
| 17 | LS | 145.31 | (0.8076) | $V_2C$ | $\underline{113}$ |
| 18 | VW | 145.99 | (0.8061) | $V_2C$ | --- |
| 19 | VVW | 153.36 | 0.7922 | ? | --- |
| 20 | LS | 156.01 | (0.7881) | ζ | |
| 21 | W | 157.01 | (0.7867) | ζ | 12 $\underline{20}$ |

Table 17. X-ray data of V-38.60 at. % C annealed at 1300°C for 220 hours

| Line | Relative intensity $I/I_o$ | Reflection angle (2θ) | Plane spacing d, Å | Phases | hkl |
|---|---|---|---|---|---|
| 1 | VW | 39.54 | 2.2773 | $V_2C$ | 100 |
| 2 | LS | 41.13 | 2.1927 | $V_2C$ | 101 |
| 3 | W | 42.54 | 2.1233 | ζ | 107 |
| 4 | LS | 54.20 | 1.6909 | $V_2C$ | 102 |
| 5 | LS | 65.06 | 1.4323 | ζ | 10 $\underline{16}$ |
| 6 | W | 72.47 | 1.3031 | ζ | 119 |
| 7 | VW | 78.02 | 1.2237 | ζ | 205 |
| 8 | VW | 78.72 | 1.2145 | ζ + $V_2C$ | 027 + 201 |
| 9 | W | 105.13 | 0.9700 | ζ | 11 $\underline{24}$ |
| 10 | LS | 111.98 | 0.9292 | ζ | 20 $\underline{20}$ |
| 11 | W | 116.-3 | 0.9066 | ζ | 21 $\underline{10}$ |
| 12 | LS | 118.19 | 0.8977 | ζ | 12 $\underline{11}$ |
| 13 | W | 123.44 | 0.8746 | ζ | 21 $\underline{13}$ |
| 14 | W | 126.96 | 0.8621 | $V_2C$ | 105 |
| 15 | LS | 145.37 | 0.8068 | $V_2C$ | 112 |
| 16 | W | 146.97 | 0.8034 | ? | --- |
| 17 | LS | 148.98 | (0.7994) | ζ | 21 $\underline{19}$ |
| 18 | W | 149.52 | (0.7983) | ζ | 21 $\underline{19}$ |
| 19 | LS | 156.04 | (0.7874) | ζ | 12 $\underline{20}$ |
| 20 | W | 156.93 | (0.7861) | ζ | 12 $\underline{20}$ |

Table 18. X-ray data of V-39.67 at. % C annealed at 1300°C for 220 hours

| Line | Relative intensity $I/I_o$ | Reflection angle (2θ) | Plane spacing d, Å | Phases | hkl |
|---|---|---|---|---|---|
| 1 | VW | 36.29 | 2.4735 | ζ | 012 |
| 2 | VS | 37.81 | 2.3786 | ζ + VC | 104 + 111 |
| 3 | VS | 39.32 | 2.2911 | ζ | 015 |
| 4 | VS | 42.44 | 2.1303 | ζ | 107 |
| 5 | VS | 44.44 | 2.0388 | ζ | 018 |
| 6 | VW | 59.22 | 1.5604 | ζ | 01 $\underline{14}$ |
| 7 | S | 63.72 | 1.4604 | ζ + VC | 110 + 022 |
| 8 | W | 68.40 | 1.3727 | ζ | 01 $\underline{17}$ |
| 9 | W | 75.24 | 1.2624 | ζ + VC | 021 |
| 10 | LS | 76.55 | 1.2446 | ζ + VC | 024 + 133 |
| 11 | LS | 77.44 | 1.2323 | ζ | 205 |
| 12 | VW | 79.55 | 1.2049 | ζ | 027 |
| 13 | VVW | 80.50 | 1.1931 | ζ + VC | 028 + 222 |
| 14 | VW | 107.97 | 0.9531 | ζ | 02 $\underline{19}$ |
| 15 | VVW | 108.97 | 0.9471 | VC | 133 |
| 16 | W | 112.12 | 0.9292 | ζ | 20 $\underline{20}$ |
| 17 | W | 113.38 | 0.9225 | ζ | 128 |
| 18 | W | 116.42 | 0.9069 | ζ | 11 $\underline{24}$ |
| 19 | S | 131.96 | 0.8465 | ζ + VC | 030 + 224 |
| 20 | W | 148.85 | 0.8003 | ζ | 21 $\underline{19}$ |
| 21 | W | 151.45 | (0.7955) | VC | 115, 333 |
| 22 | VW | 151.96 | (0.7946) | VC | 115, 333 |

Table 19. X-ray data of V-40-49 at. % C annealed at 1300°C for 220 hours

| Line | Relative intensity $I/I_o$ | Reflection angle (2θ) | Plane spacing d, Å | Phases | hkl |
|---|---|---|---|---|---|
| 1 | S | 37.87 | 2.3727 | ζ + VC | 104 + 111 |
| 2 | W | 39.23 | 2.2944 | ζ | 015 |
| 3 | W | 42.61 | 2.1200 | ζ | 107 |
| 4 | S | 43.85 | 2.0630 | ζ + VC | 018 + 002 |
| 5 | S | 64.71 | 1.4393 | ζ | 113 |
| 6 | S | 76.84 | 1.2394 | ζ | 11 $\underline{12}$ |
| 7 | S | 80.74 | 1.1892 | ζ + VC | 028 + 222 |
| 8 | W | 108.99 | 0.9463 | VC | 133 |
| 9 | S | 113.17 | 0.9228 | ζ | 128 |
| 10 | S | 132.10 | (0.8428) | ζ + VC | 030 + 224 |
| 11 | W | 132.55 | (0.8414) | ζ + VC | 030 + 224 |
| 12 | S | 151.26 | (0.7951) | VC | 115, 333 |
| 13 | W | 152.57 | (0.7929) | VC | 115, 333 |

From the metallographic and x-ray analyses of the 39.67 at. % C alloy, the ζ phase has been shown to be at or very close to this composition. Accordingly, the proposed stoichiometry of the ζ phase is $VC_{0.657}$ or $\simeq V_3C_2$, which is in agreement with Yvon and Parthè's proposed $V_4C_{3-x}$ defect structure.

4.1.3. Formation or decomposition temperature

Evidence for ζ phase decomposition in the $VC_{0.657}$ alloy was observed by thermal analysis (Figures 16 and 17). These figures represent heating curves for DTA experiments on the $VC_{0.657}$ alloy by the two different methods described previously. Several pieces of the alloy were first annealed at 1300°C for up to 220 h to convert them to ζ. Upon heating, an endothermic decomposition reaction was observed as indicated by the small break in the ΔT curves beginning at 1330 (Figure 16) and 1315°C (Figure 17). This gives some indication of the amount of energy associated with the formation or decomposition of the ζ phase and also shows that the kinetics of the reaction was very sluggish.

The average temperature at which the decomposition begins on the heating is 1320 $\pm$ 5°C whose $\pm$ 5 is the mean deviation for four successful runs shown in Table 20.

Photomicrographs of portions of the $VC_{0.657}$ alloy after heating for a period of time following the initial 1300°C anneal are seen in Figures 18 and 19. Figure 18 represents the decomposition products after heating at 1350°C for 10 h. At equilibrium two phases, $V_2C$ (~ 33%) and VC (67%) were present (Figure 18). Upon cooling, precipitation of $V_2C$ and ζ

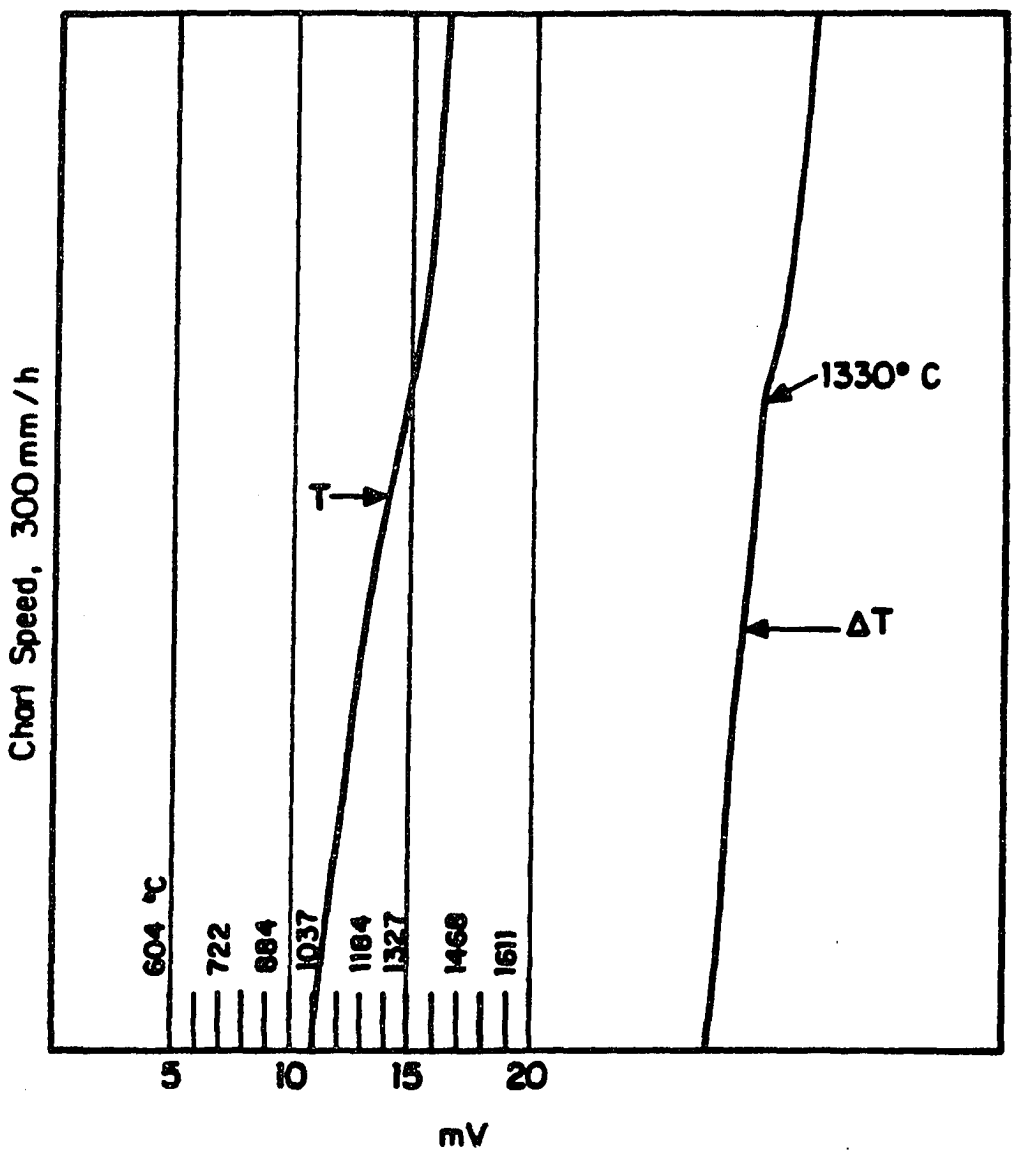


Figure 16. Typical DTA heating curve of ζ-phase alloy. Heating and cooling in NRC furnace

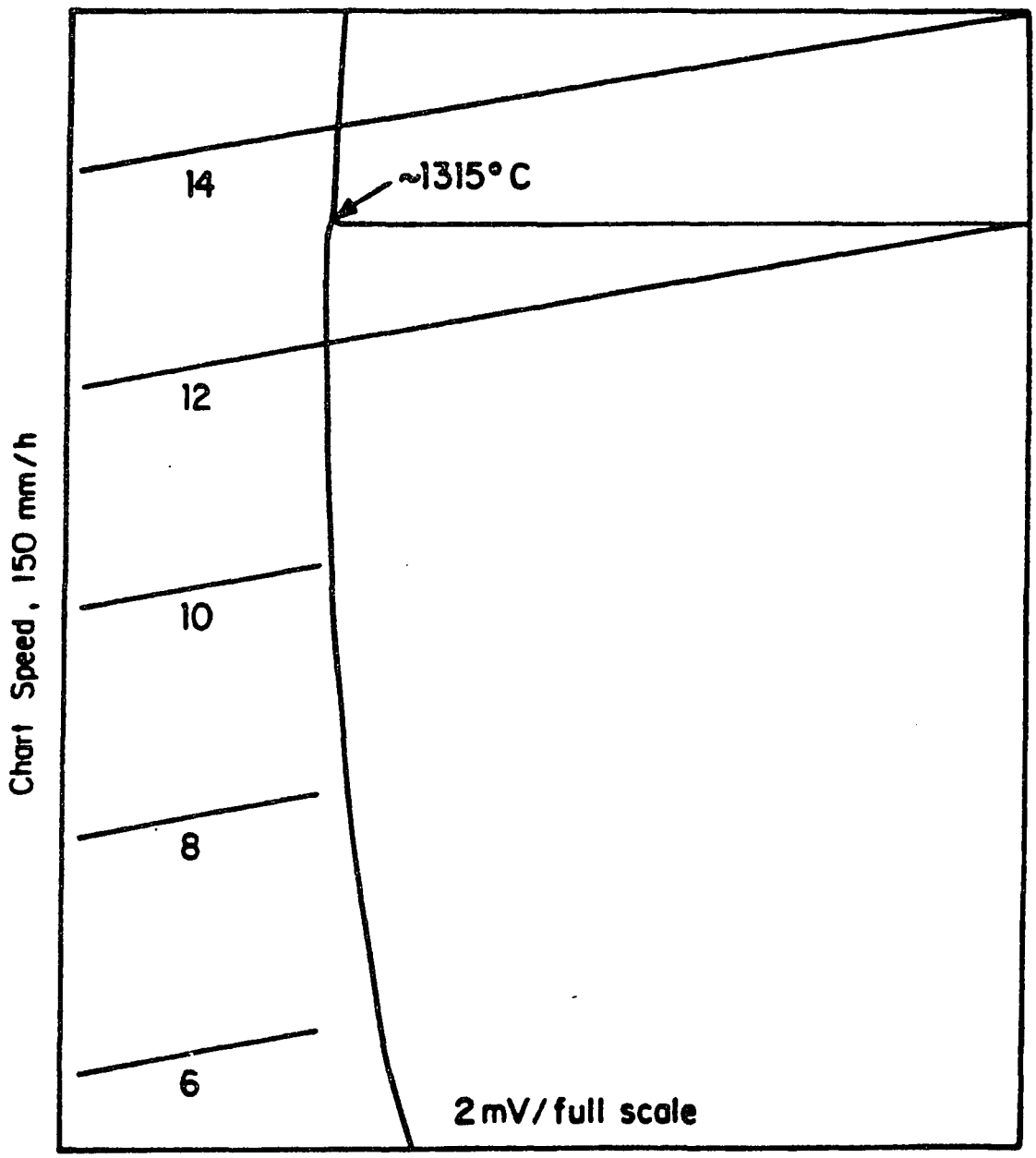


Figure 17. Typical DTA heating curve of ζ-phase alloy using Advanced Differential Thermal Analyzer

Table 20. DTA - data for ζ phase decomposition

| Sample | Annealing time, h | Evidence existence | Initial decomposition temperature, °C | Comments |
|---|---|---|---|---|
| 1 | 220 | Yes | 1330 | NRC and |
| 2 | 6 | No | -- | XY |
| 3 | 20 | No | -- | Recorder |
| 4 | 60 | Yes | 1317 | Method |
| 5 | 100 | Yes | 1322 | |
| 6 | 220 | Yes | 1315 | Advanced Differential Thermal Analyzer |

occurs giving rise to the banded or platelike structure characteristic of alloys in the VC-rich, two-phase region. A photomicrograph of this alloy after decomposition of ζ at 1450°C (Figure 19) shows a microstructure consisting predominantly of the banded VC phases. This is in agreement with the marked temperature dependence of the monocarbide phase as is seen in Figure 4.

## 4.2. Solid Solubility of C in Vanadium

A solubility determination by equilibrating a polycrystalline rod with graphite at 1300°C for 23 h gave a specimen with the microstructure, shown in Figure 20. The appearance of a continuous carbide phase along the grain boundaries raised the following question. Was this due to the

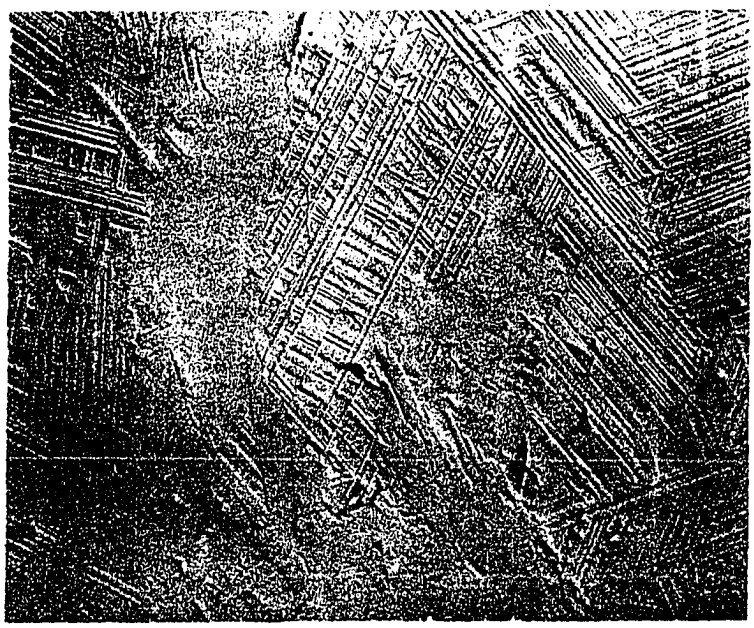

Figure 18. ζ-phase alloy heated at 1350°C for 10 h followed by furnace cooling. $V_2C$ (clear area) and VC (banded area). Chemically etched, X250

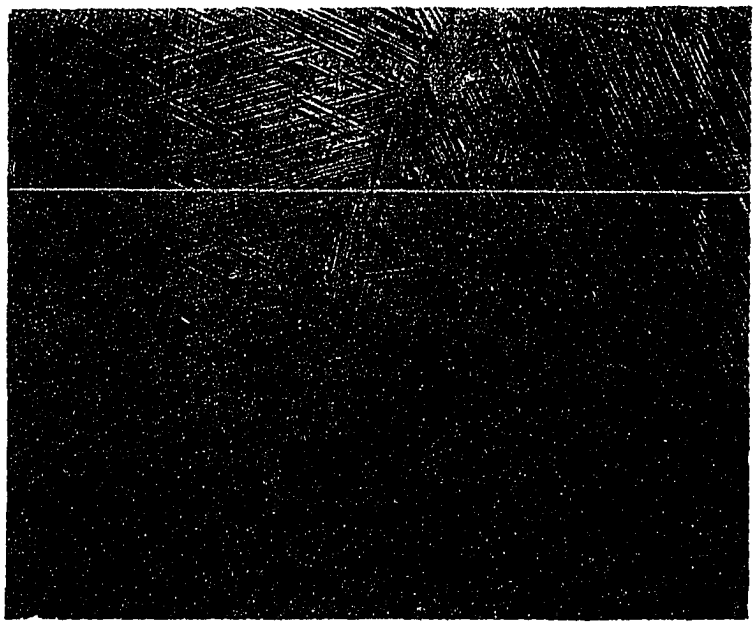

Figure 19. ζ-phase alloy heated at 1450°C. Predominantly VC at temperature. Chemically etched, X250

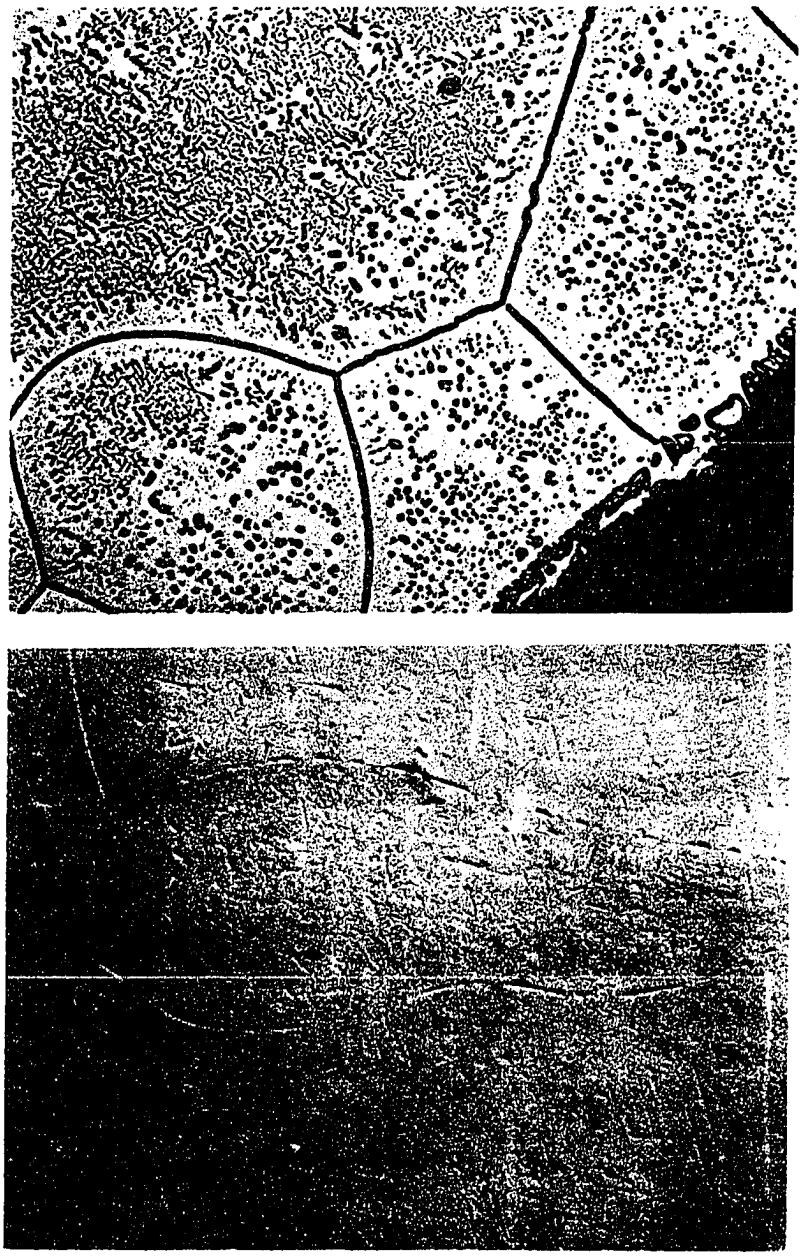


Figure 20. Polycrystalline vanadium equilibrated with charcoal at 1300°C, (a) selected area near the surface: vanadium with carbide precipitate within grains and continuous carbide phase along boundaries, X40 and (b) selected area near the center of specimen: note the discontinuous carbide phase along grain boundaries, X100. Chemically etched

Was this due to the precipitation of carbide along grain boundaries as is suggested by the depleted region near the boundaries or was some of this due to carburization along the boundaries at temperature? If the latter were the case, it would show high carbon results. For that reason, parallel experiments were run on single and polycrystalline vanadium rods equilibrated with graphite at temperatures in the range of 1300 - 1500°C. In addition, single crystal samples were equilibrated at 1100°C and 1200°C. At 1400°C, a single crystal and a polycrystalline sample were also equilibrated for a longer time, 7.5 h, in an attempt to determine whether equilibrium had been established in the earlier short time run, 5 h. As can be seen from the data at 1400°C in Table 21, the results were inconclusive. For the single crystal specimen, as the time of equilibration was increased the amount of soluble carbon at 1400°C in vanadium increased from 1.2 for 5 h to 2.1 at. % for 7.5 h. This supports the conclusion that equilibrium was not attained in the single crystal specimen in 5 h. The low result (1.5 at. % C) for the long time polycrystalline run is difficult to explain since the shorter run gave a higher result (2.0 at. % C). This low value may be due to an improper positioning of the sample in the crucible, which prevented diffusion of carbon in some portion of the surface. With the exception of this value, the overall results show a regular increase in solubility with temperature for both single and polycrystalline specimens as is seen from Table 21.

Table 21. Alloy composition and solvus temperature for V-C alloys

| Temperature °C | Equilibrating time, h | Carbon analysis, at. % | |
|---|---|---|---|
| | | Single crystal | Polycrystalline |
| 1100 | 23 | 0.1 | |
| 1200 | 14 | 0.4 | |
| 1300 | 8 | 1.1 | 1.3 |
| 1400 | 5 | 1.2 | 2.0 |
| 1400 | 7.5 | 2.1 | 1.5 |
| 1500 | 3 | 2.3 | 2.6 |

4.2.1. Solvus boundary

Two curves based on the data in Table 21 are shown in Figure 21. Separate curves are shown for the single and polycrystalline results with the higher solubility curve corresponding to the polycrystalline material. Similar results have been reported by Peter [66] for carbon in molybdenum. Micrographs of V-C alloys after equilibration of single crystal samples at 1300, 1400 and 1500°C (Figure 22) show carbide particles ($V_2C$) of increasing size and amount with increasing temperature. These alloys were a single phase at the equilibration temperature with the carbide precipitating during cooling. In the polycrystalline samples, the carbide precipitates appear to agglomerate rather rapidly and have the tendency to segregate at the boundaries of the vanadium grains as shown in Figures 23-24. In a micrograph of the polycrystalline sample (Figure 20a), it can be seen that the carbide

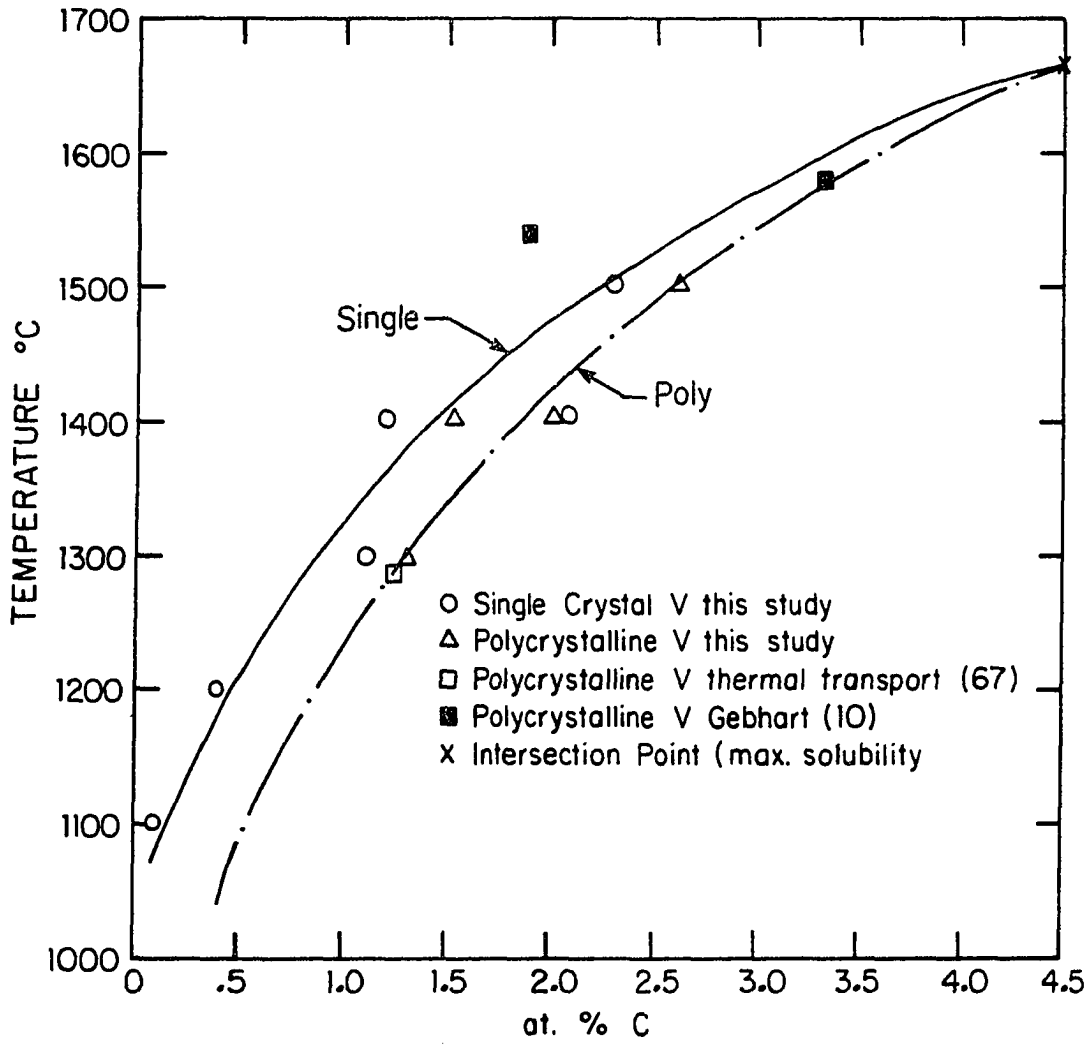


Figure 21. Plot of solubility data, T versus C (at. % C)

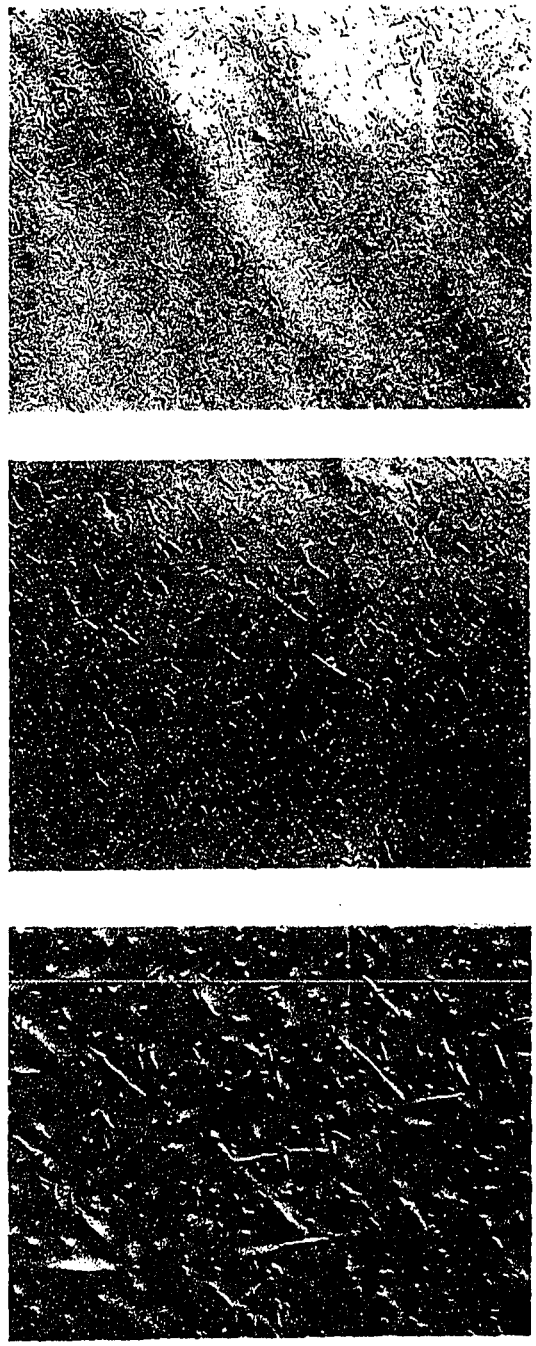


Figure 22. Single crystal vanadium samples equilibrated with fine charcoal at (a) 1300°C, (b) 1400°C and (c) 1500°C. Vanadium matrix with $V_2C$ precipitate. Chemically etched, X200

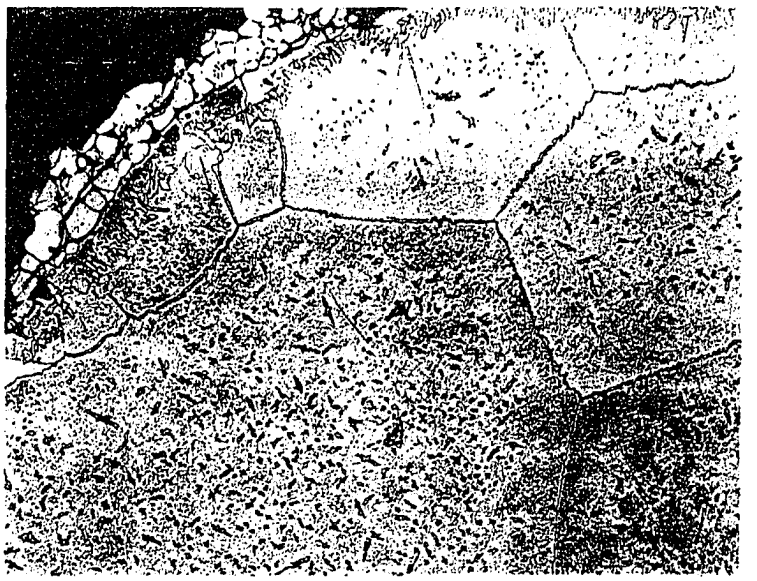

Figure 23. Polycrystalline vanadium equilibrated with charcoal at 1400°C. Vanadium with carbide precipitate within grains and segregated at boundaries. Chemically etched, X50

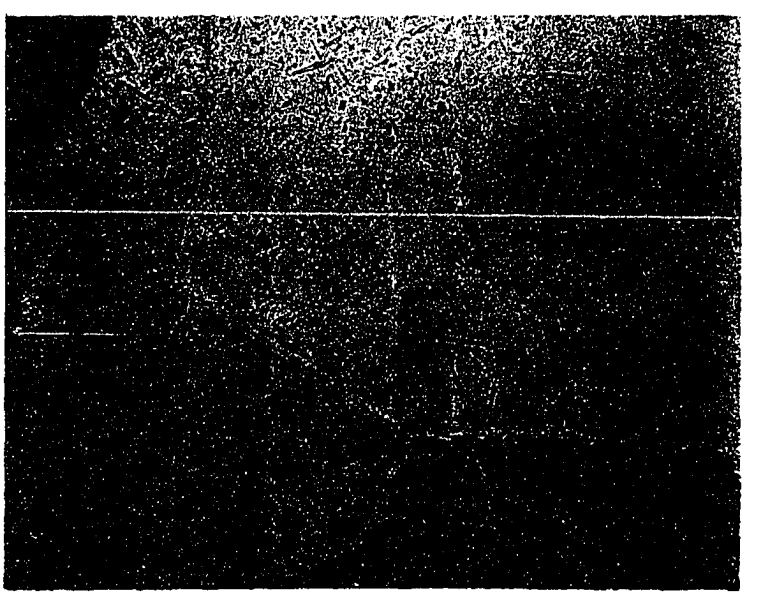

Figure 24. Polycrystalline vanadium equilibrated with charcoal at 1500°C. Carbide precipitate in vanadium matrix and segregated at grain boundaries. Chemically etched, X50

phase along the grain boundaries appears to be continuous near the surface but becomes discontinuous towards the interior (Figure 20b). This indicates that except for some penetration of carbide along grain boundaries near the surface none of the carbide phase was present at the equilibration temperature. So, it was concluded that since the boundaries enhance the carbon diffusion, the polycrystalline samples attain equilibrium faster than the corresponding single crystal samples. This is a likely explanation of why the solvus boundary for the single crystal appears to be less than for the polycrystalline sample. At the same time, the solvus curve for polycrystalline vanadium is considered to be at or near equilibrium. This conclusion was supported by data from a thermal transport study of carbon in a two phase V-C alloy [67] seen as a plotted point that lies on the polycrystalline curve of Figure 21. Okafor et al. [68] investigated the mass transport of some Fe-Ni-C two-phase alloys exposed to a temperature gradient and found a large jump in solute concentration at the temperature and concentration coinciding with a point lying on the solvus curve. Since these experiments were long time transport runs (<100 h), it seems that almost complete equilibrium should be attained. Another support comes from the agreement between the long time (7.5 h) single crystal experiment which gave 2.1 at. % C and the 5 h polycrystalline run at the same temperature which gave 2.0 at. % C. The final support comes from the 1580°C data of Gebhart et al. [10] seen as a plotted point in Figure 21. Their data point at 1530°C, however, is well below even the single crystal curve indicating that the equilibrium was not attained.

4.2.2. Heat of solution

In Figure 25, the plot of log c: (at. % C), the solubility limit for carbon as a function of $(1/T)K^{-1}$, shows a linear relationship for both single and polycrystalline material. The two straight lines were drawn using the linear least squares method as shown in Figure 25.

It can be shown from thermodynamic considerations [69] that a graphical analysis of a log $c_i$ vs $T^{-1}$ plot in Figure 25 can be represented by the relation $c_i = A \exp^{-(\Delta H/RT)}$ where $c_i$ is the atom fraction of the interstitial solute at the saturation, A is a constant for the specific system, T is the absolute temperature, R is the gas constant and $\Delta H$ is the heat of solution of the coexisting phase. If the above relation is rewritten in the form $\log c_i = \log A - (\Delta H/2.303\ R)(1/T)$, the heat of solution can be calculated from the slope $(-\Delta H/2.303\ R)$. The calculated heat of solution of C in V for the polycrystalline solvus curve is 81.6 kJ/mol (19.5 kcal/mol). This is somewhat lower than the value of 105.8 kJ/mol (25.3 kcal/mol) taken from Gebhart et al. [10] which is in fair agreement with the value of 27.9 kcal/mol obtained from the single crystal results. Since the polycrystalline curve is considered to represent more closely the equilibrium conditions, the lower value (19.5 kcal/mol) is taken as the heat of solution of carbon in vanadium.

4.2.3. Determination of maximum solid solubility

From Figure 25 it is seen that as the temperature increases the apparent solubility of carbon increases in both single and polycrystalline vanadium. The difference between the apparent amounts of carbon

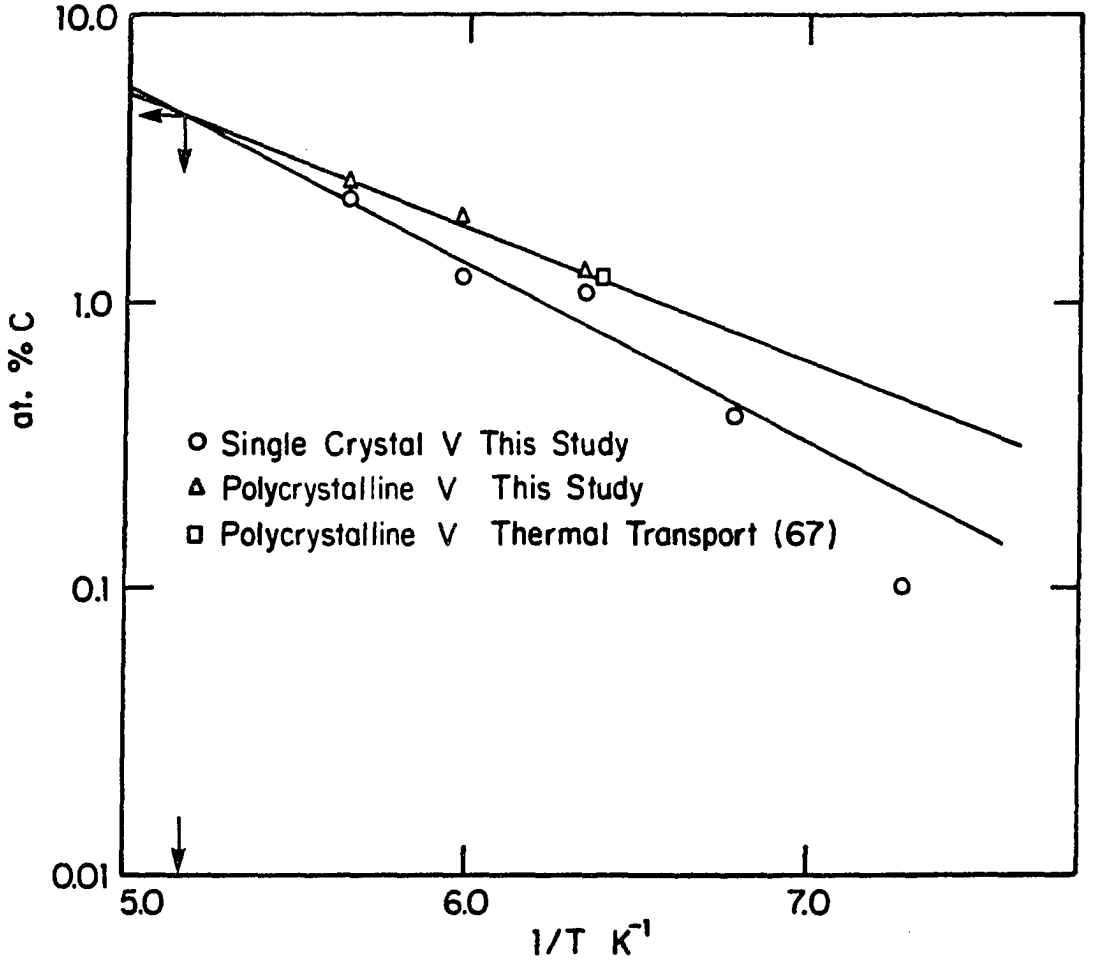


Figure 25. Least squares plot of Log C (at. % C) versus $\frac{1}{T}$

solubility in polycrystalline and single crystal vanadium decreases with temperature and should approach zero at higher temperatures where the diffusion is fast enough that equilibrium would be reached in a relatively short time in either a single crystal or a polycrystalline material. This appears to be the case at the eutectic temperature where the two lines in Figure 25 intersect at 4.5 at. % C and 1665°C which is considered the maximum solid solubility. This result agrees very well with the maximum solubility of C in vanadium reported by Tret'yachenko and Eremenko [11] at around 4.0 at. % C, Gebhart et al. [10] at 5 at. % C and Rudy et al. [5] at 5.5 at. % C.

### 4.3. Redetermination of Composition and Temperature of VC-C Eutectic

The existence of an eutectic between the vanadium monocarbide and graphite has been well-established by many investigators [5, 11, 29, 31]. In this present study, the existence of the eutectic is clearly verified as shown in the micrograph (Figure 26) of the 49.2 at. % C alloy. As the microstructure (Figure 26) appears to be entirely an eutectic mixture, its composition then, as determined from chemical analysis of this alloy, is proposed to be the composition of the VC-C eutectic. This is in good agreement with the reported value 49.5 $\pm$ 0.5 at. % C by Rudy et al. [5].

The eutectic temperature was determined by the pyro-optical pyrometer method described in the experimental procedure section. Six temperature readings of the melt-solid interface of the alloy were taken. The average of these readings is 2305 $\pm$ 6°C. Since the temperature was

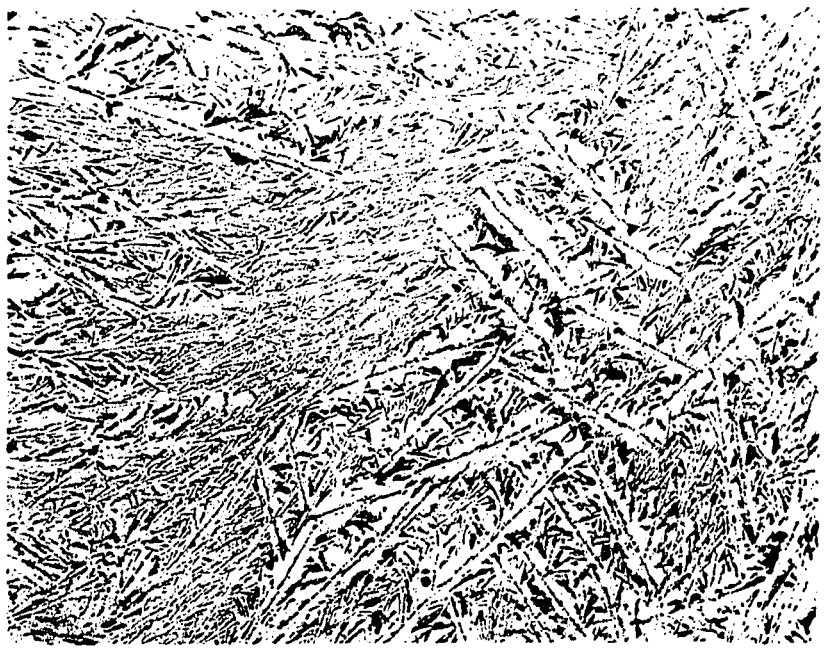

Figure 26. V-49.17 at. % C as-arc melted. 100% eutectic constituent of VC + C. Chemically etched, X250

measured by the pyrometer through a pyrex window, a sight glass correction is necessary which was determined to be 35°C.

The true temperature of the melting of the alloy T can be computed from the apparent temperature $T_a$ as indicated by the optical pyrometer from the following relation [70] if the emissivity of the alloy is known,

$$1/T - 1/T_a = \lambda \log E_\lambda/6219$$

where $\lambda$ is the wavelength of the radiation - generally red for all optical pyrometers = 0.65 micron, E is the spectral emissivity of the material and T is in K. It was assumed that the emissivity of the V-49.2 at. % C alloy is the same as that of pure molten vanadium, i.e. 0.343 [71], which gives a true melting point of the eutectic of 2720°C. Since the exact emissivity of the alloy is unknown, this introduces an uncertainty in this value estimated to be about $\pm$ 25°C.

To calibrate the technique used in this measurement, the melting point of pure zirconium was determined using the identical procedure and conditions. The melting point of the zirconium reference obtained in this way using an emissivity of 0.318 [71] for molten zirconium is 1925°C. This is higher than the actual melting point of zirconium by 75°C. This large error may be due to interference of arc radiation, although precautions were taken to eliminate this effect. Therefore, assuming the same 75°C error in the V-C alloy measurements and subtracting this value from 2720 gives the temperature of the VC-C eutectic point as 2645 $\pm$ 25°C.

## 4.4. Ordering of C in V-1.5 at. % C Alloy

Thomas and Villagrana [15] postulated the existence of a $V_{64}X$ ordered phase, where X is an interstitial atom, having a structure similar to that proposed for $Ta_{64}C$. This proposed structure is body-centered tetragonal.

An electron-micrograph of a thinned specimen from an annealed bulk specimen, 175 h at 1000°C of a 1.5 at. % C alloy, is shown in Figure 27. This micrograph shows a carbide particle in the vanadium matrix. Identification of the precipitate particle by electron diffraction was inconclusive due to the complicated diffraction pattern of matrix and precipitate obtained simultaneously (Figure 28).

Figure 29 shows an optical micrograph of the specimen annealed for 175 h at 1000°C and furnace cooled. The volume fraction of precipitate was determined by a point-counting method using superimposition of a grid over the photomicrograph. The second phase represents ~8% by volume which is consistent with the percentage of $V_2C$ is 1.5 at. % C alloy; therefore, the carbide precipitate in this alloy must be $V_2C$, not $V_{64}C$.

Figures 30a and 30b show electron diffraction patterns taken from selected areas in the matrix along the [100] and [111] directions showing four-fold and three-fold symmetry, respectively. Faint reflections indicating an ordered superlattice are evident in Figure 30b. This is probably due to an ordered body-centered tetragonal vanadium suboxide which forms lath-like precipitates (Figure 31) or the transformation twins as observed by Edington and Smallman [72] in oxidized

Figure 27. TEM micrograph for foil prepared from V-1.5 at. % C annealed bulk specimen, 175 h at 1000°C. Showing a carbide particle in vanadium matrix

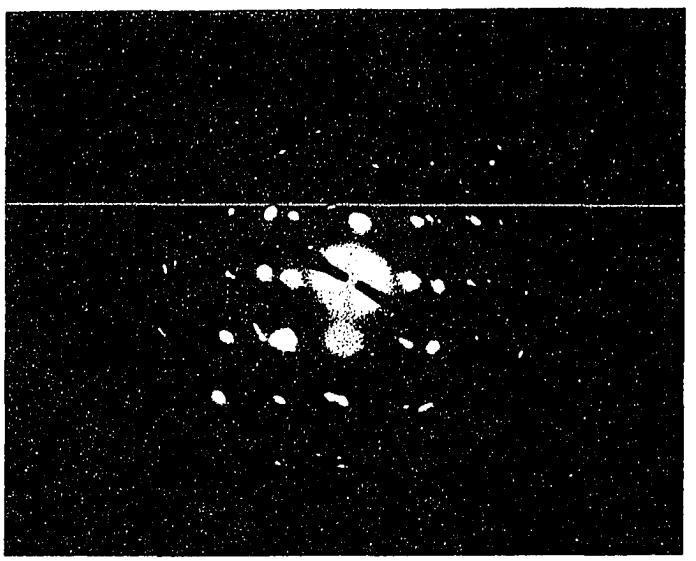

Figure 28. A selected-area diffraction pattern of precipitate and matrix obtained simultaneously. Showing complicated pattern

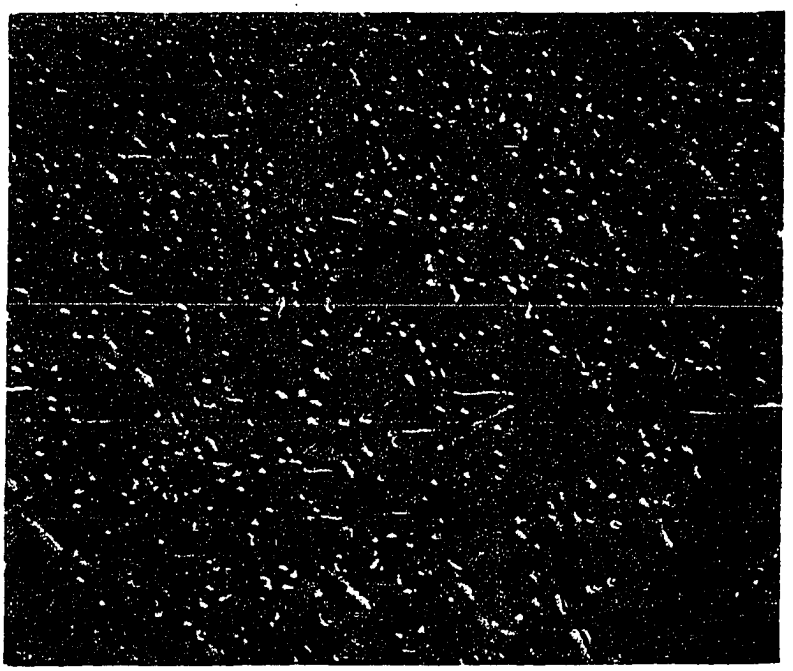

Figure 29. An optical micrograph for V-1.5 at. % C annealed bulk specimen, 175 h at 1000°C. Showing second phase (~ 8 volume %). Chemically etched, X800

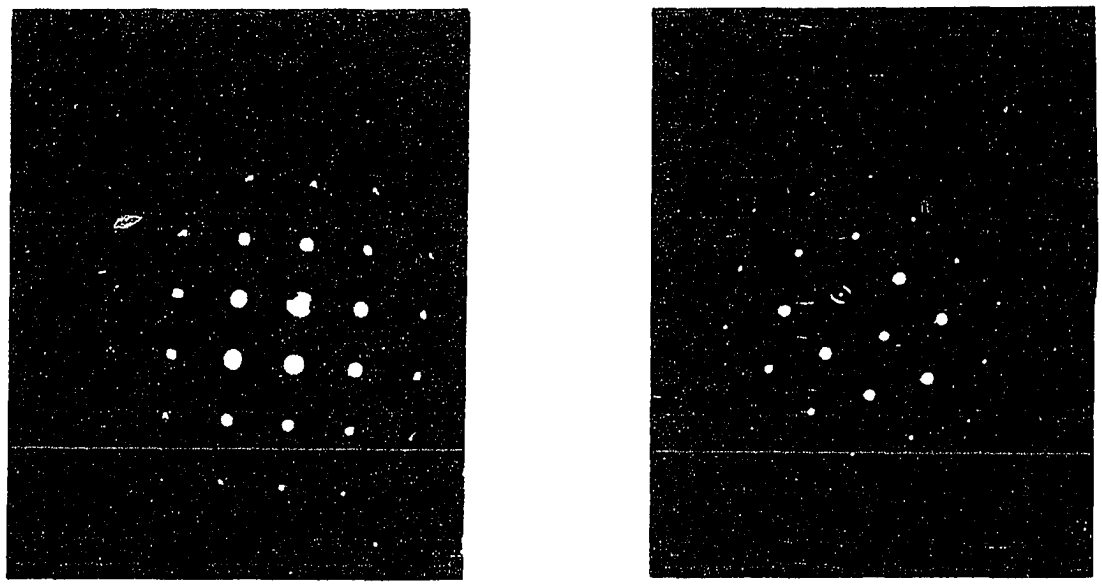

(a) (b)

Figure 30. A selected-area diffraction of matrix. Showing (a) [100] and (b) [$\bar{1}$11] orientations

Figure 31. TEM micrograph of foil used in Figure 27 but different area. Showing lath-like precipitate

vanadium bulk specimens at low air pressures. From the above results, it is concluded that there is no dilute ordered phase $V_{64}C$, since the first equilibrium carbide phase appears to be $V_2C$. Other evidences from the literature supporting this conclusion will be discussed below.

Diercks and Wert [73] found metastable coherent precipitates in a quenched and aged (300-450°C for 1 h) specimen of 0.2 at. % C which appears to have a bcc structure closely related to that of the V matrix. Upon isochromal aging at higher temperatures (550-600°C for 1 h), the coherent precipitate transforms to semicoherent carbide precipitate of the equilibrium phase, $V_2C$. Recently, Dahmen and Thomas [74] showed that the $Ta_{64}$ ordered phase was actually the ordered suboxide $Ta_{12}O$ resulting from absorption of oxygen by the material under the experimental conditions. Additional evidence against an ordered $V_{64}C$ phase comes from the low solubility of C in V at 1000°C (~0.25 at. % C). This is incompatible with ordering of $V_{64}C$ in the V matrix.

### 4.5. Residual Resistivity Ratio Study

The resistivity of a metal containing impurity atoms may be written in the form [75]

$$\rho = \rho_l + \rho_i \qquad \text{(Eq. 1)}$$

where $\rho_l$ is the resistivity caused by thermal motion of the lattice, and $\rho_i$ is the resistivity caused by scattering of the electron waves by impurity atoms. The residual resistivity (RR) as $T \to 0$ is caused mainly by electron-impurity scattering $\rho_i$ where $\rho_l$ vanishes as $T \to 0$. The residual resistivity ratio (RRR) of a specimen is usually defined as the

ratio of its resistivity at room temperature to its resistivity at liquid helium $\rho_{(298K)}/\rho_{(4.2K)}$.

For a more precise relation, the above equation may be expanded to include the physical defects $\rho_d$, and defects from electron-surface scattering $\rho_s$ as [76]:

$$\rho = \rho_l + \rho_i + \rho_d + \rho_s \ . \qquad \text{(Eq. 2)}$$

Therefore, for a more precise determination of the contribution of impurities alone, the specimens should be large to eliminate the surface effect and well-annealed to eliminate the effect of physical defects (vacancies, dislocations and grain boundaries).

The residual resistivity caused by homogeneously distributed impurities is proportional to their concentration $n_i$ and the relation may be written as:

$$\rho_i = (\rho_i/n_i) \times n_i = \rho'_i \times n_i \ . \qquad \text{(Eq. 3)}$$

As $\rho_i$ is the summation of the individual contributions to the residual resistivity and referring to the definition of RRR, the following relation can be derived for the major interstitial impurities, Si, O, N and C, in vanadium:

$$RRR = \rho(V)_{298}/\rho_{Si} + \rho_O + \rho_N + \rho_C \ . \qquad \text{(Eq. 4)}$$

The above equation is also based on the assumption that the contribution of the substitutional impurities such as Al, Fe, Ta and W to the residual resistivity $\rho_i$ is so small that it can be neglected. From Equations (3)

and (4):

$$RRR = \rho(V)_{298}/\rho_{Si}\,\rho'_{Si} + n_O\rho'_O + n_N\rho'_N + n_C\rho'_C \,. \qquad \text{(Eq. 5)}$$

The above equation was used to calculate the $\rho'_C$ from known values for $\rho'_{Si}$, $\rho'_O$, $\rho'_N$ and chemical analyses for the above elements. The value of $\rho(V)_{298} = 22.6 \times 10^{-6}$ ohm-cm was calculated from the measurement of the resistance of sample 1 in Table 22 at the room temperature. The values of $\rho'_{Si} = 8.5$ ohm cm/at. ppm [77], $\rho'_O = 5.2$ ohm cm/at. ppm [78] and the assumption that $\rho'_O = \rho'_N$ were used for the calculation of $\rho'_C$. The measured values of RRR for different specimens and the corresponding calculated $\rho'_C$ are listed in Table 22.

As shown in the table, the calculated values of $\rho'_C$ obtained from unannealed samples (2, 3, and 4) show the largest discrepancies and this leads to some doubt regarding the assumption that the $\rho_d$ term in Equation (2) was constant in all the cold-worked samples. Hence, it was concluded that the physical defect term $\rho_d$ may contribute differently to the resistivity of each specimen.

The average value of $\rho'_C$ is $5.2 \pm 2.9 \times 10^{-10}$ ohm-cm/at. ppm where $2.9 \times 10^{-10}$ is the arithmetic mean deviation. Since the deviation from the mean for specimen 2 is greater than the arithmetic mean by a factor of 2.5, that value can be disregarded. An average value of $4.0 \pm 1.9 \times 10^{-10}$ ohm-cm/at. ppm is obtained for $\rho'_C$ based on the six remaining data points.

The expected value of $\rho'_C$ is about the same order as for $\rho'_O$ or $\rho'_N$, but it may be larger or smaller. For example, values of $\rho'_C = 4.3$,

Table 22. Measured RRR and calculated $\rho'_C$ for alloys of different compositions

| Specimen | Impurity Elements in at. ppm | | | | $\Gamma_{4.2}$ | $\rho'_C \times 10^{-10}$ ohm-cm/at. ppm | Remarks |
|---|---|---|---|---|---|---|---|
| | Si | O | N | C | | | |
| 1 | 10[a] | 111[a] | 36[a] | 251[a] | 103 | 5.38 | |
| 2 | 10 | 235 | 100 | 565[a] | 25.4 | 12.51 | as cold rolled |
| 3 | 10 | 235 | 100 | 1010[a] | 22.6 | 8.09 | " " " |
| 4 | 10 | 235[a] | 100[a] | 2331[a] | 24.7 | 3.14 | " " " |
| 5 | 415[a] | 181[a] | 255[a] | 530[a] | 29.3 | 3.52 | annealed at 1000°C for 3 h |
| 6 | 415 | 190 | 255 | 1060 | 26.9 | 2.41 | " " " |
| 7 | 415 | 190 | 255 | 1910 | 24.9 | 1.69 | " " " |

[a]Analyzed composition.

$\rho'_N = 5.2$, and $\rho'_O = 4.5 \times 10^{-10}$ ohm-cm/at. ppm in niobium were reported by Schulze [76].

In Table 23, the average value of $\rho'_C$ as obtained in the present investigation is compared with those reported by early workers for different metals.

Table 23. Comparison of $\rho'_C$ obtained from different metals

| Metal | $\rho'_C \times 10^{-10}$ ohm-cm/at. ppm | Reference |
|---|---|---|
| V | $4.0 \pm 1.9$ | Present study |
| Nb | 4.3 | [76] |
| Th | 2.85 | [79] |

# 5. CONCLUSIONS

## 5.1. Proposed Phase Diagram of the V-C System

The proposed phase diagram of the V-C system shown in Figure 32 is based on the diagram of Rudy et al. (Figure 1) with several modifications. Rudy's diagram that was proposed in 1968 is chosen because it is still rather widely accepted. The modifications include mainly the results of the present investigation and data from the literature on order-disorder transition reactions in $V_2C$ and VC-phase regions.

The major features of the proposed phase diagram (Figure 32) can be described as follows.

### 5.1.1. Pure vanadium

The melting point of pure vanadium is taken as 1910 $\pm$ 7°C. This value is based on a critical evaluation by Hultgren et al. [9].

### 5.1.2. Vanadium-rich solvus

The vanadium-rich solvus is based on the experimental results of this investigation. These results are based on the solid solubility study of carbon in polycrystalline vanadium as discussed in a previous section. The maximum solubility of carbon in vanadium was obtained from extrapolation of the poly and single crystal vanadium data (Figure 25) which gives 4.5 at. % C at 1665°C. This is proposed as the maximum solubility of C in vanadium and is in good agreement with the literature data.

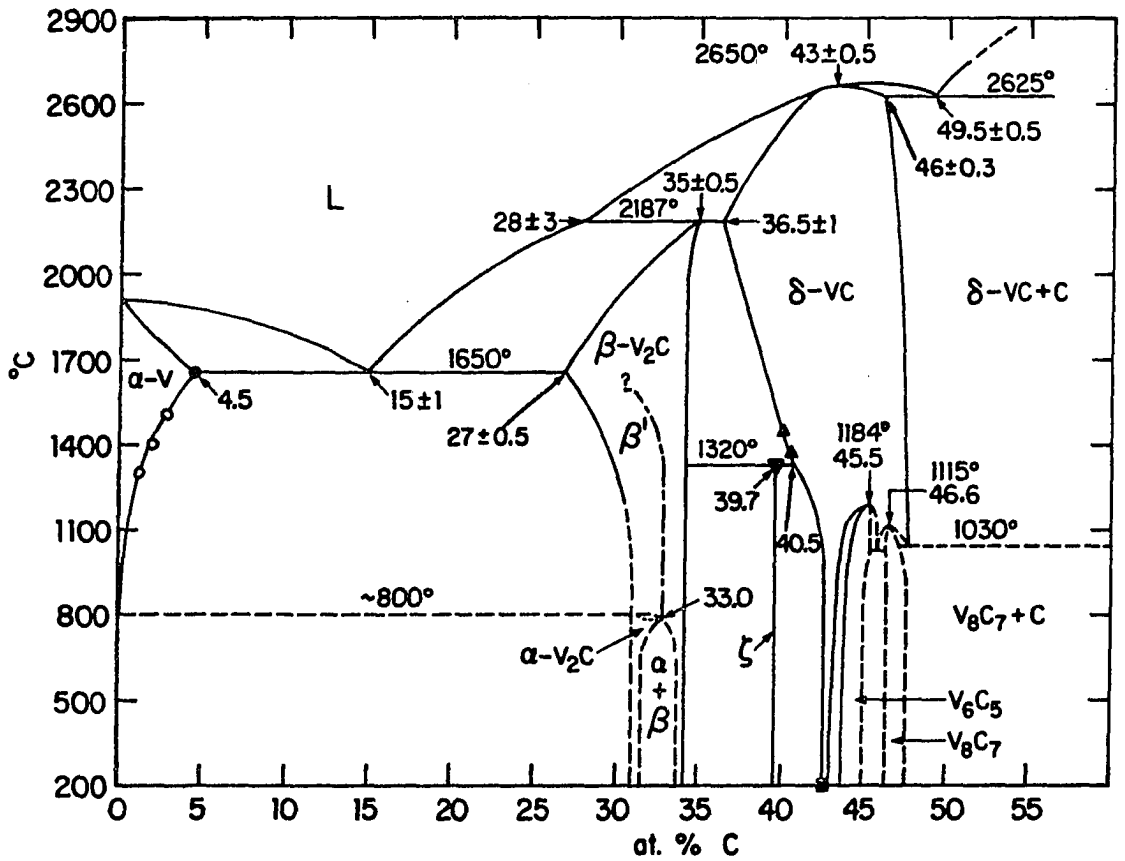


Figure 32. Proposed phase diagram of V-C system based on literature data and experimental results.

- o Polycrystalline solubility study
- ● Extrapolation of poly and single crystal data
- ▼ DTA
- ▲ Metallography
- ■ X-ray and metallography

5.1.3. $V_2C$ phase

All features of this phase are the same as in Rudy's diagram except for one modification and changes in phase designation. The phase at high temperature is designated as $\beta$-$V_2C$ and at low temperatures as $\alpha$-$V_2C$. Arbuzov et al. [21] and Khaenko and Fak [22] proposed the existence of an ordered hexagonal $V_2C$ phase ($\beta'$) with a composition range of 31 to 33.0 at. % C upon quenching from 1600°C. They also postulated that the $\beta'$ phase transforms to an orthorhombic phase that is identified as $\beta_p$ at $\sim$ 800°C and 33.0 at. % C. The $\beta_p$ phase is considered as another designation for the $\alpha$-$V_2C$ phase which is shown in the phase diagram. The boundary of $\beta'$ is questionable as shown in Figure 32.

5.1.4. Zeta phase

The decomposition temperature of the $\zeta$ phase was determined in this investigation as 1320 $\pm$ 5°C using a differential thermal analysis technique. The stoichiometry of this phase was also determined in this investigation using the chemical analysis for carbon in the $\zeta$ phase alloy. This gives the stoichiometric composition $\sim V_3C_2$ for the phase which is in good agreement with literature data.

The crystal structure and lattice parameters obtained from this investigation confirm the results of Yvon and Parthè [26] who proposed a hexagonal structure for the phase with a = 2.917 $\pm$ 0.001 A and c = 27.83 $\pm$ 0.01 A and c/a = 9.541.

5.1.5 VC phase

Several modifications of Rudy's proposed VC phase region are included in the diagram (Figure 32). According to microstructural evidence obtained in this investigation, the low-carbon boundary of this phase was modified in the range of 1300 - 2187°C. From metallographic and x-ray analyses in this investigation for the V-42.98 at. % C alloy, a point on the high-carbon boundary of VC phase at room temperature was obtained.

The ordered compounds $V_6C_5$ and $V_8C_7$ are based on the results of Billingham et al. [43] and Emmons and Williams [36]. The version proposed by Billingham et al. is chosen in preference to the others in Figure 2 for the following reasons:

1) The transformation reactions for $VC_{0.833} = V_6C_5$ and $VC_{0.875} = V_8C_7$ are shown as first-order reactions in Figure 2c. This agrees with the results of Shacklette and Williams [44, 45] who found evidence for a first-order transformation from their electrotransport studies and the results of Emmons and Williams [36] from thermodynamics of order-disorder transformations in vanadium carbide investigation. Khaenko and Fak [22] reported a second-order reaction $\delta'_m = \delta'_c$ (Figure 2a).
2) Storms et al. [29] showed the ordered compounds, $V_6C_5$ and $V_8C_7$, but not in a complete form. They did not show boundaries for $V_6C_5$ and represented $V_8C_7$ as a line compound that is formed by a peritectoid reaction at $\simeq$ 1130°C.

The temperatures of the order-disorder transformations for $V_6C_5$ and $V_8C_7$ are shown as 1184 ± 12 and 1112 ± 8°C based on the results of Emmons and Williams [36] who used a differential thermal analysis. These values are based on very recent results obtained from an advanced DTA technique. Also their transition temperature of $V_6C_5$ is in good agreement with other literature data.

5.1.6. VC-C eutectic

The 49.5 ± 0.5 at. % C value for the VC-C eutectic is based on the results of Rudy et al. The chemical analysis of the eutectic alloy prepared in this investigation was 49.2 at. % C which falls in the range of Rudy's value. Tret'yachenko's results gave 49.9 at. % C, which can be considered in agreement with Rudy's value, while Adelsberg and Cadoff [31] claimed a value of 53.5 at. % C which is quite different from the other results.

The temperature of the VC-C eutectic which is also based on Rudy's results is 2625 ± 12°C. The temperature obtained from this investigation is 2645 ± 25°C which is in agreement with Rudy's value within the limits of uncertainty. It is also in agreement with the value of Adelsberg and Cadoff, 2670°C, but differs considerably from Tret'yachenko's value of 2750°C.

## 6. SUMMARY

1. A comprehensive survey of the published literature on the V-C system was made. Available crystal structure data and thermodynamic properties of the reported vanadium carbide phases were compiled and evaluated.

2. The $\zeta$ phase of this system was prepared by annealing a 39.67 at. % C alloy at 1300°C for 220 hours in a vacuum furnace. The crystal structure was determined as hexagonal with a = 2.9185 $\pm$ 0.002 A and c = 27.788 $\pm$ 0.03 A. The decomposition temperature was determined by DTA as 1320 $\pm$ 5°C.

3. The vanadium-rich solvus was determined from a series of equilibration experiments. A maximum solubility of 4.5 at. % C at 1665°C was obtained. The heat of solution of carbon in vanadium was determined to be 81.6 kJ/mol (19.5 kcal/mol).

4. The composition and temperature of the VC-C eutectic were determined as 49.2 at. % C and 2645 $\pm$ 25°C, respectively.

5. Attempts were made to confirm the postulated existence of ordered $V_{64}C$, but no evidence was found to support this postulation.

6. The contribution of carbon to the residual resistivity of vanadium was calculated from measurements of residual resistivity ratio (RRR) as a function of carbon content. A value for $\rho'_C(\Delta\rho_C/\Delta n_C)$ of $4.0 \pm 1.9 \times 10^{-10}$ ohm-cm/at. ppm was obtained from this calculation.

7. A phase diagram of V-C system is proposed based on a combination of data from the literature and the reported experimental results.

## 7. REFERENCES


1. Lye, R. G.; Hollox, G. E.; Venables, J. R. In "Anistropy in Single Crystal Refractory Compound"; Vahldiek, F. W.; Mersol, S. A., eds.; Plenum Press: New York, 1968; Vol. 2, Chapter 7.

2. Hollox, G. E. Mat. Sci. Eng. 1968, 3, 121.

3. Kieffer, R.; Braun, H. "Vanadin. Niob. Tantal"; Springer-Verlag: Berlin, 1963; Chapter 7.

4. Storms, E. K.; McNeal, R. J. J. Phys. Chem. 1962, 66, 1401.

5. Rudy, E.; Windisch, S.; Bruck, C. E. Planseeber. Pulvermet. 1968, 16, 3.

6. Smith, J. F. Bull. of Alloy Phase Diagrams 1981, 2(1), 40.

7. Wilhelm, H. A.; Carlson, O. N.; Dickinson, J. M. J. Met. 1954, 6, 915.

8. Oriani, R. A.; Jones, T. S. Rev. Sci. Instrum. 1954, 25, 248.

9. Hultgren, R.; Orr, R. L.; Andrseson, P. D.; Kelly, K. "Selected Values of Thermodynamic Properties of the Elements"; John Wiley: New York, 1963; 302.

10. Gebhart, E.; Fromm, E.; Roy, U. Z. Metallkde. 1966, 57, 682.

11. Tret'yachenko, L. A.; Eremenko, V. N. Izv. Akad. Nauk SSSR, Neorg. Mater. 1966, 2, 1586.

12. Matheus, D. R.; Rowe, E. A. U.S. Bur. Mines Rep. Invest. 1968, No. 6628.

13. Schonberg, N. Acta Chem. Scand. 1954, 8, 624.

14. Gurevish, M. A.; Ormont, B. F. Zh. Neorg. Khim. 1957, 7, 1633.

15. Thomas, G.; Villagrana, R. E. Acta Metall. 1966, 14, 1633.

16. Brauer, G.; Schnell, W. D. J. Less-Common Met. 1964, 7, 23.

17. Yvon, K; Nowotny, H. and Kieffer, R. Mh. Chem. 1967, 98, 34.

18. Nowotny, H.; Beneskovsky, F. Planseeber. Pulvermet. 1968, 16, 204.

19. Yvon, K.; Rieger, W.; Nowotny, H. Mh. Chem. 1966, 97, 699.

20. Rudy, E.; Brakl, C. E. J. Amer. Chem. Soc. 1967, 50, 265.

21. Arbuzov, M. P.; Fak, V. G.; Khaenko, B. V. Izv. Akad. Nauk SSSR, Neorg. Mater. 1976, 12, 846.

22. Khaenko, B. V.; Fak, V. G. Izv. Akad. Nauk SSSR, Neog. Mater. 1978, 14, 1294.

23. Brauer, G.; Lesser, R. Z. Metallkde. 1959, 50, 8.

24. Lesser, R.; Brauer, G. Z. Metallkde. 1958, 46, 622.

25. Rasserts, Von H.; Benesovsky, F.; Nowotny, H. Planseeber. Pulvermet. 1966, 14, 178.

26. Yvon, K.; Parthè, E. Acta Crystallog. 1970, B26, 149.

27. Billingham, J.; Lewis, M. H. Philos. Mag. 1971, 24, 231.

28. Van Landuyt, J.; Amelinckx, S. Colloq. Inter. C.N.R.S. 1972, 205, 87.

29. Storms, E. K.; Lowe, E.; Baca, E.; Griffin, J. High Temp. Sci. 1973, 5, 276.

30. Rudy, E.; Progulski, G. Planseeber. Pulvermet. 1967, 15, 13.

31. Adelsberg, L. M.; Cadoff, L. H. J. Am. Ceram. Soc. 1968, 51[4], 213.

32. Rudy, E.; Rudy, El.; Benesovsky, F. Planseeber. Pulvermet. 1962, 10, 42.

33. Volkova, N. M.; Alyamovskii, S. I.; Geld, P. V. Izv. Akad. Nauk SSSR, Metallurgiya i Cornoe Delo. 1963, 5, 134.

34. DeNovion, C. H.; Lorenzelli, R.; Costa, P. Compt. Rend. 1966, B263 775.

35. Froidevaux, C.; Rossierr, D. J. Phys. Chem. Solids 1967, 268, 1197.

36. Emmons, G. H.; Williams, W. S. J. Mater. Sci. 1983, 18, 2589.

37. Venables, J. D.; Khan, D.; Lye, R. G. Philos. Mag. 1968, 18, 177.

38. Hollox, G. E.; Venables, J. D. Trans. Japan Inst. Met. 1968, 9, 295.

39. Govila, R. K. Acta Metall. 1972, 20, 447.

40. Billingham, J.; Bell, P. S.; Lewis, M. H. Philos. Mag. 1972, 25 661.

41. Hiraga, K. Philos. Mag. 1973, 27, 130.

42. Khaenko, B. V. Izv. Akad. Nauk SSSR, Neorg. Mater. 1979, 15, No. 11, 1952.

43. Billingham, J.; Bell, P. S.; Lewis, M. H. Acta Crystallog. 1972, A28, 602.

44. Shacklette, L. W.; Williams, W. S. J. Appl. Phys. 1971, 42, 4698.

45. Shacklette, L. W.; Williams, W. S. Phys. Rev. 1973, B7, 5041.

46. Bowman, A. L.; Wallace, T. C.; Yernel, J. I.; Wenzel, R. J.; Storms, E. K. Acta Crystallog. 1965, 19, 6.

47. Schomate, C. H.; Kelly, K. K. J. Am. Chem. Soc. 1949, 71, 314.

48. Hultgren, R.; Desal, P. D.; Hawkins, D. T.; Gleiser, M.; Kelley, K. K. "Selected Values of the Thermodynamic Properties of Binary Alloys"; American Society for Metals: Metals Park, Ohio, 1967; p. 532.

49. Chernyaev, V. S.; Schhetnikov, E. N.; Krentsis, R. P.; Geld, P. V. Izv. Akad. Nauk SSSR, Neorg. Mater. 1967, 3, 789.

50. Barin, I., Knacke, O. "Thermochemical Properties of Inorganic Substances"; Springer-Verlag: Berlin, 1973; p. 833.

51. King, E. G. J. Am. Chem. Soc. 1949, 71, 316.

52. Storms, E. "The Refractory Carbides"; Academic Press: New York, 1973; Chapter 4.

53. Volkova, N. M.; Gel'd, P. V.; Alyamovskii, S. I. Zh. Neorg. Khim. 1965, 10, 187.

54. Alekseev, V. I.; Shvartsman, L. A. Doklady Akad. Nauk SSSR 1960, 133, 1331.

55. Worrel, W. L. J. Phys. Chem. 1964, 68, 954.

56. Reznitskii, L. A. Russian J. Phys. Chem. 1966, 40, 68.

57. Pillai, P. V. S.; Sundareson, M. Trans. Indian Inst. Met. 1957, 28, No. 4, 319.

58. Gurevich, M. A. J. Inorg. Chem. USSR (Engl. Transl.) 1963, 8, 1378.

59. Worrel, W. L.; Chipman, J. J. Phys. Chem. 1964, 68, 860.

60. Mah, A. D. U.S. Bur. of Mines 1966, Report No. 6177.

61. Fujishiro, S.; Gokcen, N. A. J. Electrochem. Soc. 1962, 109, No. 9, 835.

62. Kohl, F. J.; Stearns, C. A. J. Phys. Chem. 1970, 40, 2760.

63. Sallivan, T. A. J. Met. 1956, 17, 45.

64. Carlson, O. N.; Schmidt, F. A.; Krupp, W. E. J. Met. 1966, 18, 320.

65. Power, R. W.; Margaret, V. D. Acta Metall. 1958, 6, 643.

66. Peter, B. Ph.D. Thesis, Bergakademi Freiberg, Germany, 1978.

67. Uz, M.; Carlson, O. N. Ames Laboratory, 1983 (unpublished work).

68. Okafor, I. C.; Carlson, O. N.; Martin, D. M. Metall. Trans. 1982, 13A, 1713.

69. Darkin, L. S.; Gurry, R. W. "Physical Chemistry of Metals"; McGraw Hill: New York, 1969; Chapter 16.

70. Kehl, G. L. "The Principals of Metallographic Laboratory Practice"; McGraw Hill: New York, 1949; Chapter 8.

71. Bonnell, D. W.; Treverton, J. A.; Valerga, A. J.; Margrave, J. L. In "Temperature-Its Measurements and Control in Science and Industry"; Plum, H. H., ed.; Instrument Soc. of Amer.: Pittsburgh, 1972; Vol. 4, Part 1, Chapter 2.

72. Edington, J. W.; Smallman, R. E. Acta Metall. 1965, 13, 155.

73. Diercks, D. R.; Wert, C. A. Metall. Trans. 1972, 3, 1699.

74. Dahmen, U.; Thomas, G. SCR Metall. 1979, 13, 527.

75. Kittel, C. "Introduction to Solid State Physics"; 4th ed.; John Wiley: New York, 1971; Chapter 7.

76. Schulze, K. J. Met. 1981, 5, 33.

77. Carlson, O. N.; Schulze, K. Max Planck Inst. Fur Metall., Germany, 1983. (Unpublished Work.)

78. Bresseys, J.; Greten, R.; Vanholseke, G. J. Less-Common Met. 1975, 39, 7.

79. Peterson, D. T.; Schmidt, F. A. J. Less-Common Met. 1971, 24, 233.

## 8. ACKNOWLEDGMENTS

I owe special thanks to Professor O. N. Carlson for his knowledgeable guidance, thought-provoking discussions and critical analysis in the preparation and completion of this investigation. I wish to thank F. A. Schmidt for supplying the vanadium metal and for his technical suggestions. I also owe special thanks to L. P. Lincoln for his technical assistance in preparing samples and performing experiments. Many thanks are due to L. K. Reed, A. D. Johnson, M. E. Thompson and G. T. Wheelock for their help during the sample preparation. Many thanks are also due to H. H. Baker for metallographic work, J. E. Ostenson for measuring the residual resistivity ratios, R. Z. Bachman for carbon chemical analysis, A. Pelton and F. C. Laabs for their help and invaluable discussion on TEM work, T. R. Kelly and D. W. Sailsbury for their graphic arts services; as well as Dr. K. A. Gschneidner's group, especially S. Y. Yeh, for their help during performing the x-ray experiments. Thanks to all my friends, especially Dr. O. N. Carlson's group, for their help in different ways.

I would also like to thank Barbara Dubberke for an excellent job of typing my dissertation on such short notice. Finally, I would like to thank my wife, Amina, for her support and endless encouragement.